ANNALES SOCIETATIS GEOLOGORUM POLONIAE
ROCZNIK POLSKIEGO TOWARZYSTWA GEOLOGICZNEGO

v. 52—1/4: 305—333, 1982 Kraków 1984

Jan A. CZUBEK, Marta BUNIAK, Jerzy ŁOSKIEWICZ, Joanna BOGACZ, Jerzy DĄBROWSKI, Andrzej LENDA, Tomasz ZORSKI

STATISTICAL AND GEOSTATISTICAL CHARACTERISTICS OF SOME FORMATIONS IN THE CARPATHIAN FLYSCH

(29 Figs.)

Statystyczna i geostatystyczna charakterystyka niektórych formacji karpackiego fliszu

(29 fig.)

Jan A. Czubek, Marta Buniak, Jerzy Łoskiewicz, Joanna Bogacz, Jerzy Dąbrowski, Andrzej Lenda, Tomasz Zorski: Statistical and geostatistical characteristics of some formations in the Carpathian Flysch. Ann. Soc. Geol. Poloniae 52-1/4: 305—333, 1982 Kraków.

Abstract: The aim of the paper is to establish relations between geostatistical image provided by laboratory core analyses and geophysical image as represented by field logging data. Once these relations are found it is possible to construct calibration curves. This procedure is of special interest in the case when the logging probes were not previously standarized in calibration models.

The analysis of the applicability of formulas relating core and logging data has been performed for a few Carpathian flysch series of the upper Cretaceous, Paleocene and Eocene ages.

The rock matrix densities are obtained using correlations between rock porosities and their bulk density. Furthermore we obtained the shale density which for upper Cretaceous and Paleocene series was equal to 2.65 but for the Eocene series containing some carbonates the shale density was found to be equal to 2.80.

The variograms of porosity correspond in the high porosity regions to spherical scheme whereas in low porosity region we encountered rather the de Wijsian scheme. The variograms of neutron log and natural gamma logs furnished information on the shale intrinsic scheme which is of spherical type but with range of ~10 meters i.e. far larger than in the porosity case.

Key words: Carpathian Flysch, geostatistics, geophysics Jan A. Czubek, Marta Buniak, Jerzy Łoskiewicz, Joanna Bogacz, Jerzy Dąbrowski: Institute of Nuclear Physics, ul. Radzikowskiego 152, 31-342 Kraków, Poland.

Andrzej Lenda: Institute of Nuclear Physics and Techniques, Academy of Mining and Metallurgy, al. Mickiewicza 30, 30-059 Kraków, Poland.
Tomasz Zorski: Institute of Exploration Geophysics and Oil Geology, Academy of Mining and Metallurgy, al. Mickiewicza 30, 30-059 Kraków, Poland.

manuscript received: December, 1980 **accepted: January, 1981**

Treść: Celem pracy jest znalezienie związków pomiędzy obrazem geostatystycznym opartym na wynikach analiz próbek rdzeni wiertniczych i obrazem geofizycznym otrzymanym z danych profilowań radiometrycznych. Po znalezieniu tych zależności staje się możliwe wyznaczenie krzywych cechowania. Taka procedura jest specjalnie interesująca w przypadku, gdy sondy radiometryczne nie były cechowane w odpowiednich standaryzatorach.

Analiza stosowalności wzorów wiążących dane z rdzeni wiertniczych i z profilowania radiometrycznego została wykonana dla kilku serii fliszu karpackiego należących do eocenu, paleocenu i górnej kredy.

Gęstości matrycy skalnej otrzymywane były za pomocą korelacji pomiędzy porowatością i ciężarem objętościowym skał. Ponadto otrzymaliśmy gęstości iłów wypełniających pory dla utworów górnej kredy i paleocenu, które wynoszą 2,65 g/cm^3 natomiast dla utworów eocenu zawierających domieszki węglanów, gęstość iłu była równa 2,80 g/cm^3.

W obszarze wysokich porowatości wariogramy porowatości odpowiadają schematowi sferycznemu, natomiast dla obszaru małych porowatości napotykaliśmy raczej schemat de Wijsa. Z wariogramów profilowania neutronowego i naturalnego promieniowania gamma otrzymaliśmy informację dotyczącą schematu dla zailenia, który jest typu sferycznego, ale o zasięgu 10 m, tj. dużo większym niż w przypadku porowatości.

1. INTRODUCTION

The geostatistical system of the well logging data interpretation (Bogacz et al. 1979) needs some statistical and geostatistical characteristics of formation parameters. Here an example of such characteristics for the Carpathian Flysch series of the upper Cretacous, Paleocene and Eocene ages is presented.

The data are coming from a region stretching from the neighbourhood of Limanowa up to Brzozów-Rymanów area. It has been divided into two distinct geographic regions:

1. Słopnice-Limanowa region shown in Fig. 1; it measures circa 12×6 kilometers.
2. Gorlice-Jasło-Krosno-Brzozów region measuring circa 72×20 kilometers.

In the second region 28 boreholes have been situated at the Potok Fold (circa 12×2 kilometers which is shown in Fig. 2). A very short description of the borehole sample data available for these two regions is given in Table 1. About 20 cubic centimeters has been used as the

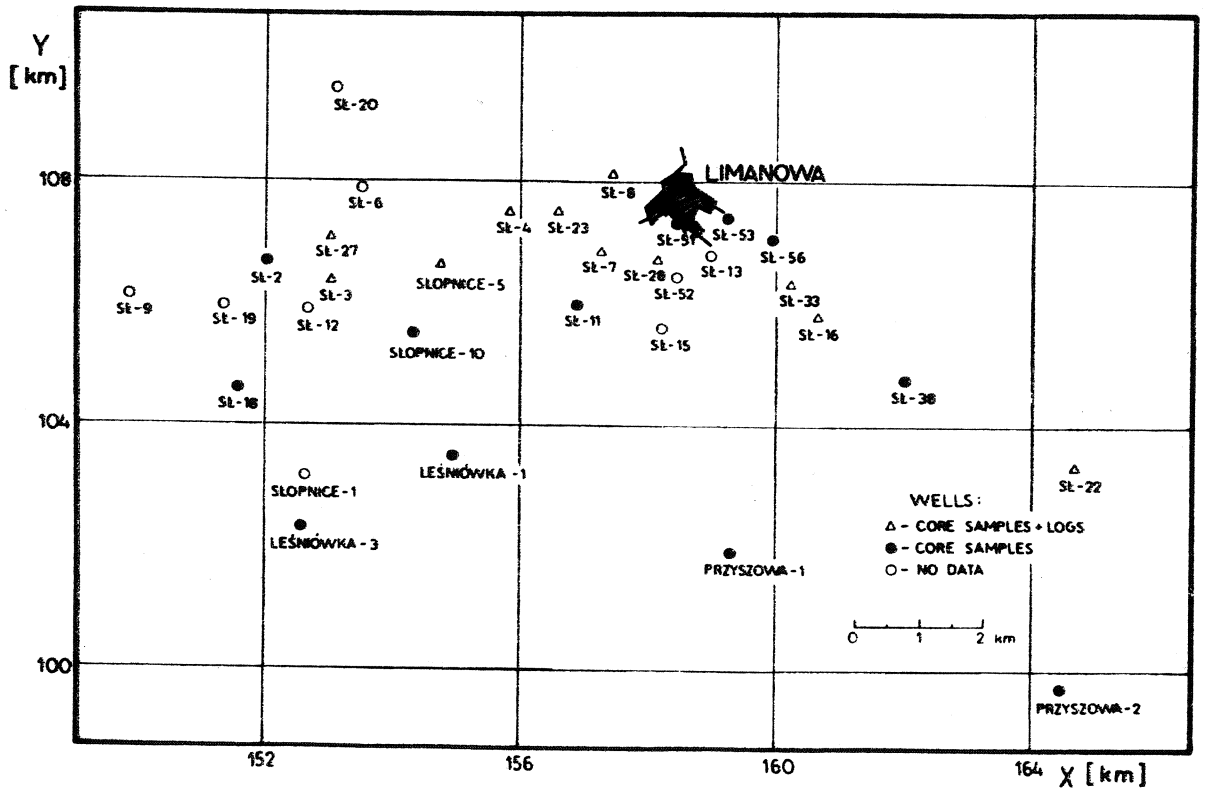

Fig. 1. Słopnice — Limanowa region

Fig. 1. Rejon Słopnice — Limanowa

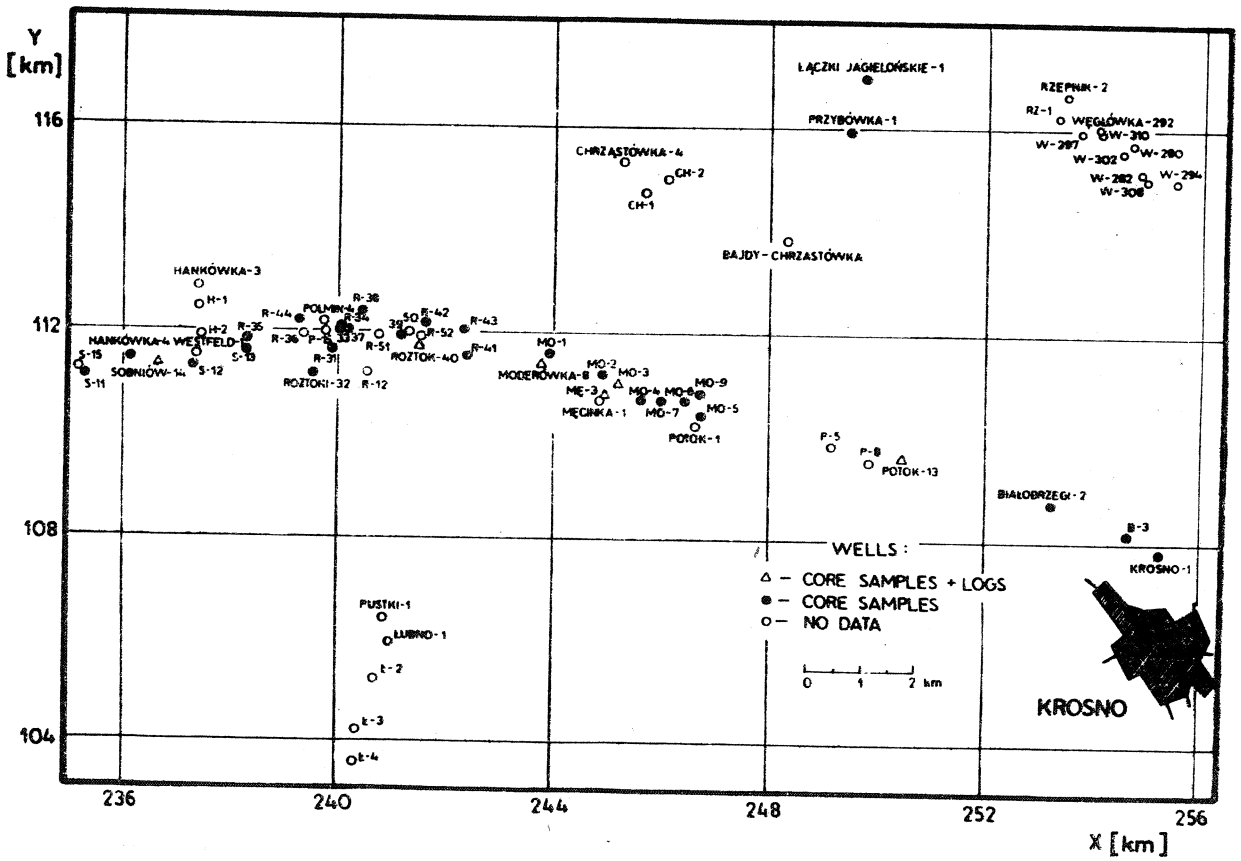

Fig.2. Potok Fold region

Fig. 2. Rejon Fałdu Potoka

standard volume for each sample taken from the core for the laboratory measurements. The x, y coordinates of each borehole have been known as well as the depth below the sea level at which each core sample has been taken out.

For some boreholes the gamma-ray, neutron-gamma and the caliper logs have been also available in the digital form. These logging data have been also pretreated to obtain the nuclear tool responses in cpm not influenced by the logging speed, ratemeter time constant and the apparatus dead time. For the natural gamma-ray log the data have been also pre-interpreted to be not influenced by the borehole diameter, gamma-ray absorption in the borehole fluid, and the radioactivity of the neighbouring layers. From the neutron-gamma ray log the gamma-ray background has been subtracted. These nuclear well logging data have been known as the averaged values for the one meter intervals along the borehole depth

All these data, the laboratory and the logging ones, have been submitted to the statistical and to the geostatistical analysis to get some characteristic parameters for the formations listed in Table 1.

Table 1

Core data available for the Carpathian Flysch

	Region:	
	Słopnice—Limanowa	Gorlice—Jasło—Krosno—Brzozów (Potok Fold incl.)
Litho-stratigraphic description	Eocene age. Krosno layers (KO), and Grzybow shales and Cergowa sandstones (GC). Sandstones, shales, mudstones.	Paleocene and Upper Cretaceous ages. Istebna layers and Czarna Rzeka shales. Sandstones and shales of the series A, B, C and D.
No. of boreholes	25	63
No. of layers	82	203
No. of samples for:		
porosity	675	1914
dry bulk density	675	709
permeability	—	816
olay content	140	122

2. TREATMENT OF THE LABORATORY DATA

The statistical distributions of the laboratory data have been calculated first. They have been fitted to the normal or to the log-normal distributions. Average value, the second and the third central moments

have been calculated, together with the histograms and the cumulative distributions. Here the abscissae have been expressed in the experimentally observed standard deviation units around the average value, whereas the cumulative distribution have been presented onto the Gaussian scale.

POROSITY

None of the mentioned above distributions fitted well the experimental data, if taken for the whole regions. Much better fit has been obtained when the data corresponding to the well defined litho-stratigraphic series were treated within the radius of about 10 km. As an example the distribution of the porosity Ø for the sandstone B of the Western part of the Potok Fold is given in Fig. 3. Here, the experimental distribution fits well the normal distribution within the 95 per cent confidence belt (which is given as the two dotted lines in this and in all forthcoming figures concerning the distributions). The same situation for the Słopnice

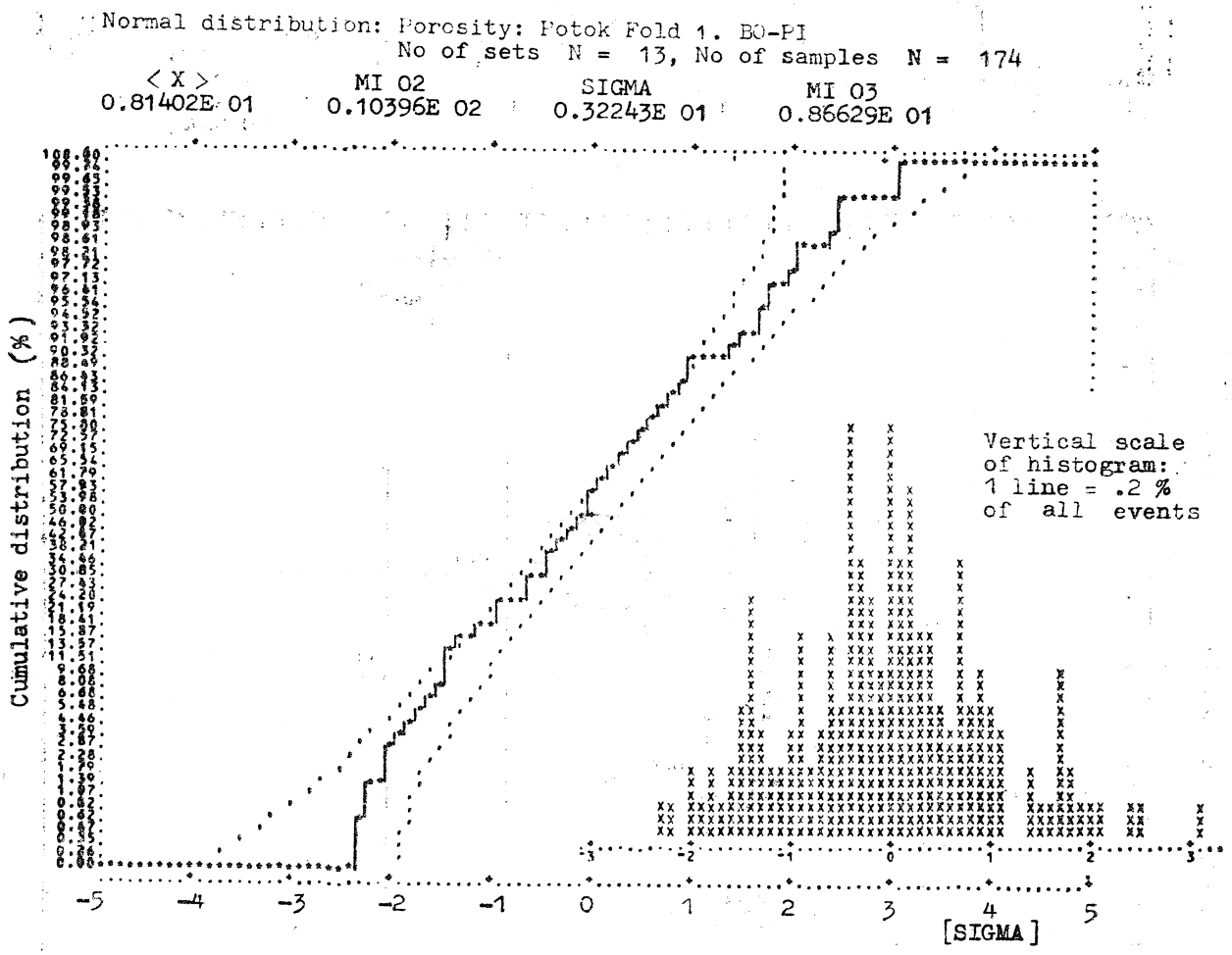

Fig. 3. Porosity distribution for sandstones B from the Potok Fold

Fig. 3. Rozkład współczynnika porowatości dla piaskowców B z rejonu Fałdu Potoka. Pionowa skala histogramu: 1 linia = 0,2% wszystkich przypadków

Log-normal distribution: Porosity. Slopnice Region. Sandstone KO
No of sets: N= 8 , No of samples N= 110

<X>	MI 02	SIGMA	MI 03
0.90209E-02	0.47870E 00	0.69188E 00	-0.15841E 00

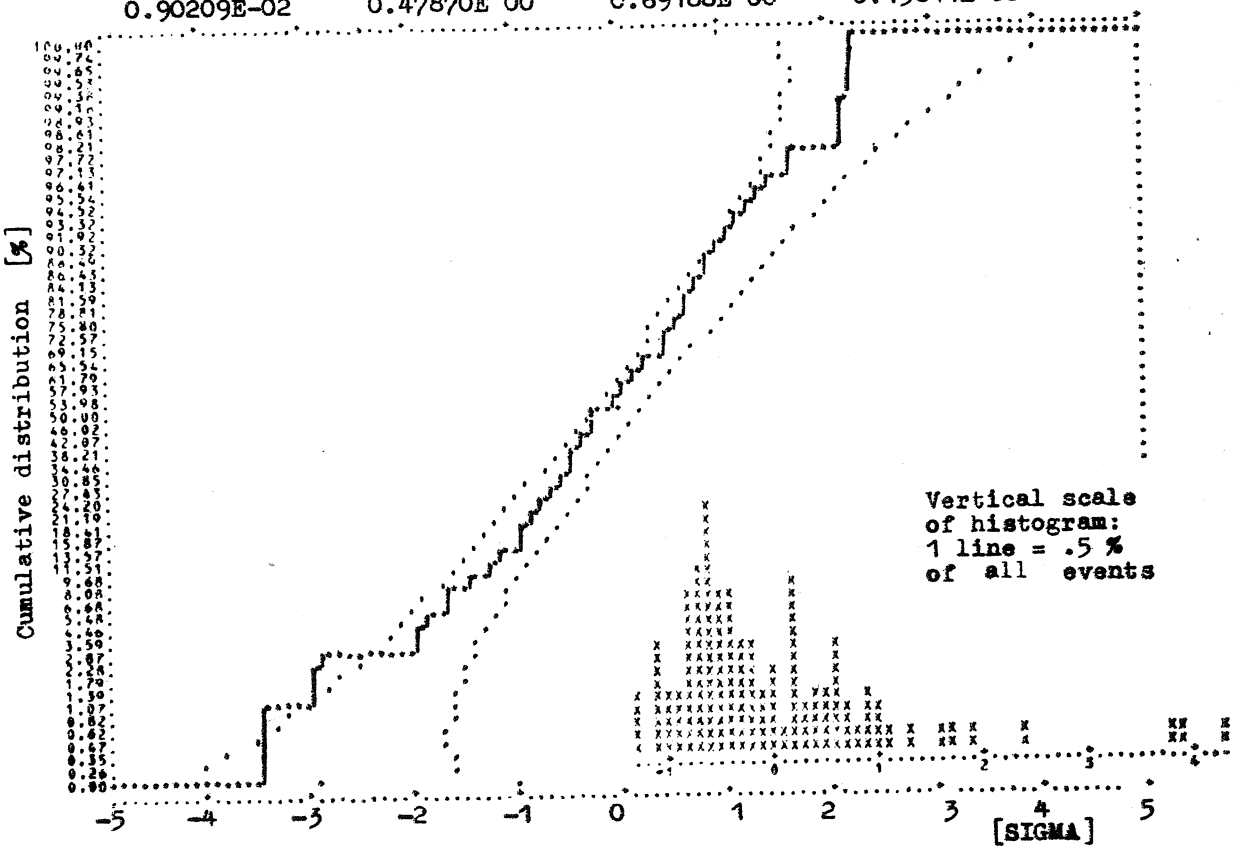

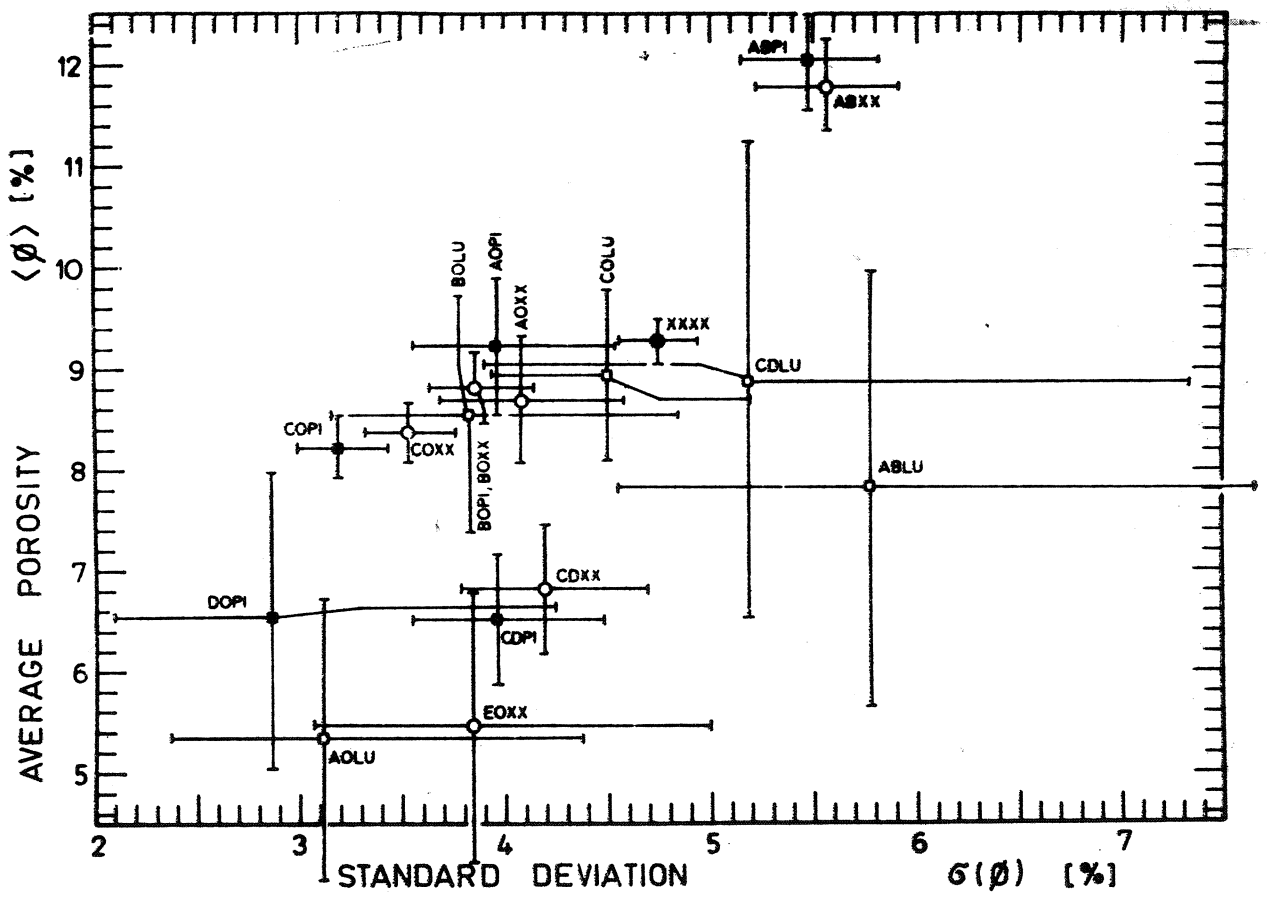

Fig. 4. Porosity distribution for sandstones KO from the Słopnice region

Fig. 4. Rozkład współczynnika porowatości dla piaskowców KO z rejonu Słopnic. Pionowa skala histogramu: 1 linia = 0,5% wszystkich przypadków

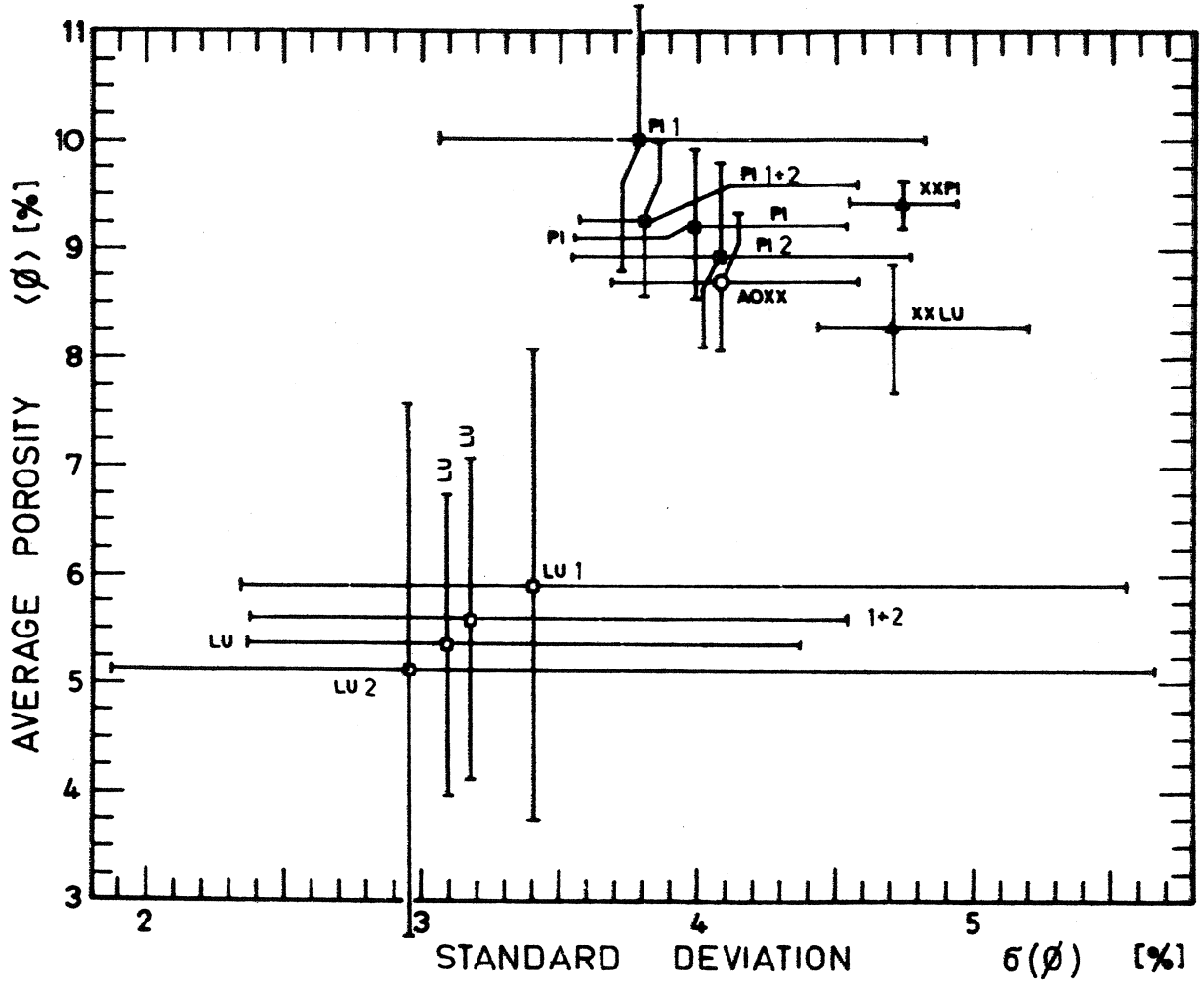

Fig. 6. Parameters of the normal distributions of the porosity for the series A in the Potok Fold region. 1 and 2 refer to the W and E parts of the Fold, respectively

Fig. 6. Parametry normalnych rozkładów współczynnika porowatości serii A rejonu Fałdu Potoka. Indeksy 1 i 2 odnoszą się odpowiednio do części zachodniej i wschodniej Fałdu

Fig. 5. Parameters of the normal distributions of the porosity for the shale/sandstone series of the Gorlice—Brzozów region (including the Potok Fold)

Fig. 5. Parametry normalnych rozkładów współczynnika porowatości serii łupków i piaskowców rejonu Gorlice—Brzozów (wraz z Fałdem Potoka)

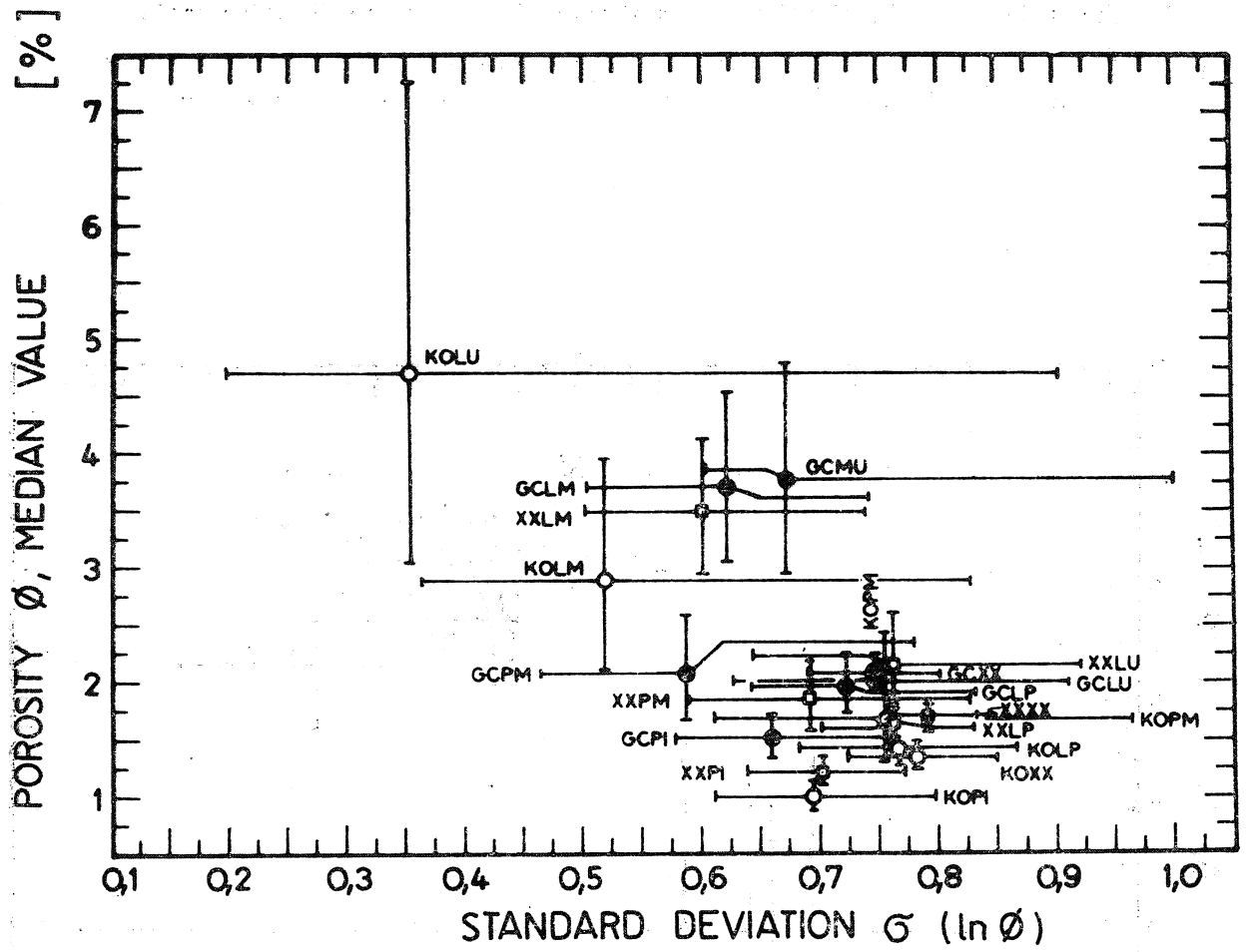

Fig. 7. Parameters of the log-normal porosity distributions for the Słopnice region. PM, LP and MU stand for different shaliness of the KO or GC sandstones (PI) or shales (LU)

Fig. 7. Parametry logarytmiczno-normalnych rozkładów współczynnika porowatości dla rejonu Słopnice. PM, LP, LM i MU oznaczają różny stopień zailenia piaskowców (PI) i łupków (LU) serii KO i GC

region is given in Fig. 4. Here the porosity fits better the log-normal distribution (the histogram in this figure is given in the linear scale, however). To be able compare the different sets of data, the estimated parameters of these distributions have been plotted in the following coordinate system: expected value $\langle Ø \rangle$ vs. the standard deviation $\sigma(Ø)$. The 95 per cent confidence belt for each estimated value has been also plotted. These data are plotted in Fig. 5. for the litho-stratigraphic series for the whole Gorlice-Brzozów region, whereas in Fig. 6. this situation is given for the series A only. In the last figure the A series have been split inside the Potok Fold into the western (1) and eastern (2) parts in view to be able to get some idea about the homogeneity of the data. Here, and in all forthcoming figures, the PI stands for sandstone, LU for shales, LP, PM, MU are the different types of the shaly sandstones, and XX neglects all lithology or stratigraphy indexes. When the rectangles of the confidence belts around each poin in this kind of presentation are, even partially, overlapping, we are not able to tell (at the 95 per cent of the

confidence level) that the two sets have been taken out from different general populations (or that they are essentially different). In this respect, for example, the shales of the series A (marked as AOLU) are not essentially different from the sandstones of the series D (marked as DOPI) in Fig. 5. The same is valid for the sandstones of the series A (marked as PI) taken from different parts of the Potok Fold (cf. Fig. 6). The confidence belts for the shale distributions (marked as LU) are always larger than these one for the sandstones (marked as PI) because of much poorer sample statistics.

The same situation for the Słopnice region is given in Fig. 7. for the median value of porosity vs. the standard deviation of $\ln Ø$.

As we can see from these figures, each small region is more or less homogeneous with, however, big differences between the regions. Moreover, the accuracy of the laboratory measurements on the core samples does not permit, in many cases, to distinguish between the different series. For this reason it is statistically allowed, at this stage of the statistical recognition of this region, to put together some sets of data belonging to different series for the further considerations, because they are not statistically different. This situation can be changed, of course, if more measurement data will be available.

DRY BULK DENSITY

Dry bulk denstiy δ_s of sandstones for the Gorlice-Brzozów region follows quite well the normal distribution (cf. Fig. 8.), whereas for the Słopnice region this agreement is not so good. For the whole set of the δ_s data for the Słopnice region the distribution is given in Fig. 9., whereas for the shale only from this region — in Fig. 10.

When one uses this kind of data to plot, for a given litho-stratigraphic series in a given region, the expected δ_s value against the expected porosity Ø value (with the 95 per cent confidence belts), the apparent mineralogical density $\tilde{\delta}_M$ can be obtained according to the formula

$$\delta_s = (1 - Ø) \cdot \tilde{\delta}_M \tag{2.1}$$

This situation for the Słopnice region is given in Fig. 11, whereas for the Potok Fold region in Fig. 12. One obtains very easily that in the first case $\tilde{\delta}_M = 2.72$ g/ccm, whereas for the second region is $\tilde{\delta}_M = 2.65$ g/ccm.

These data can be now compared with the mineralogical composition of the investigated rocks. This is done in Fig. 13, where for the Słopnice region (the KO and GC series) and for the Potok Fold (series C: shales COLU and sandstones COPI) the distribution of data, in the triangle system: quarz + feldspar, carbonates and clay minerals, is done. Assuming the mineralogical densities δ_M for quarz + feldspar, carbonates and

Normal distribution: Dry bulk density: Potok Fold. Sandstone, XX-PI
No of sets: N= 98 , No of samples N = 621

<X>	MI 02	SIGMA	MI 03
0.23982E 01	0.28038E-01	0.16745E 00	-0.45086E-02

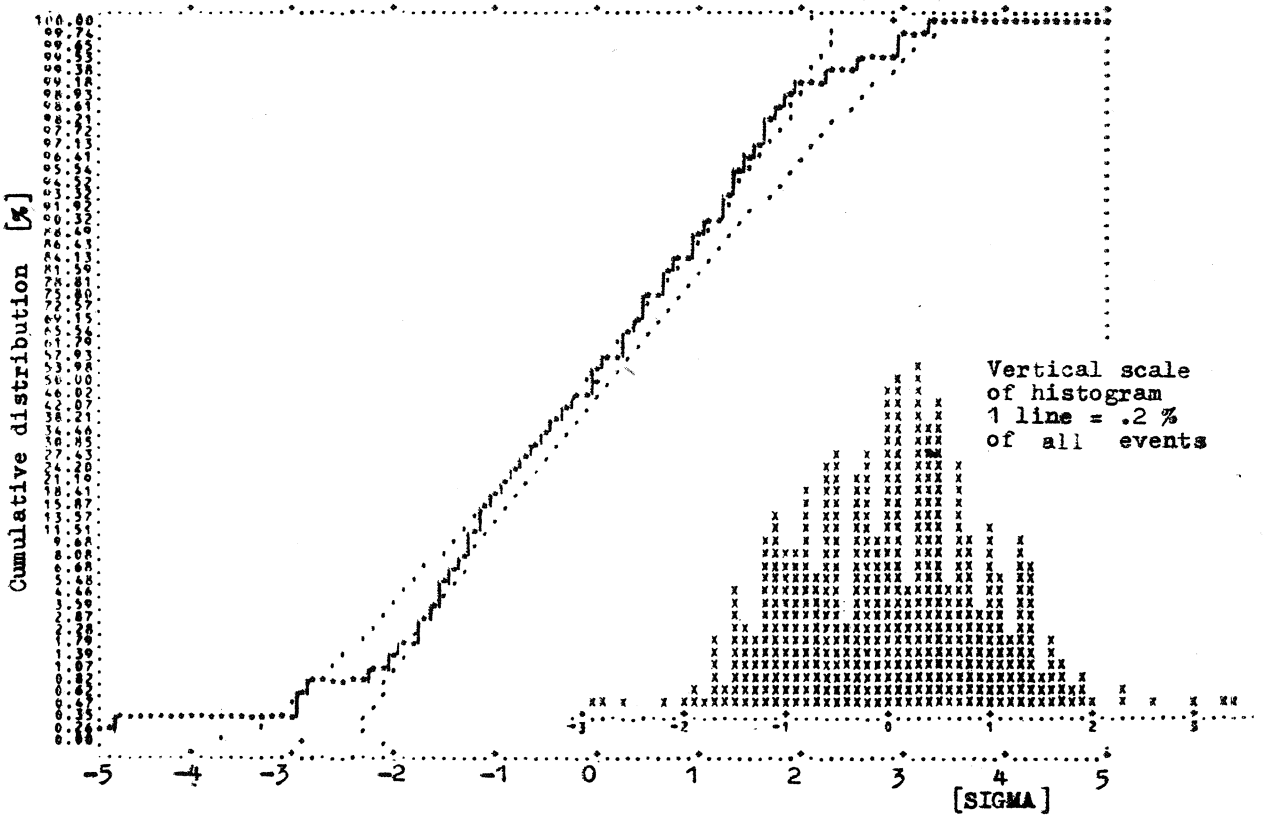

Normal distribution: Dry bulk density: Slopnice Region. XX-XX
No of sets: N= 79 , No of samples N= 675

<X>	MI 02	SIGMA	MI 03
0.26585E 01	0.51629E-02	0.71853E-01	-0.56929E-03

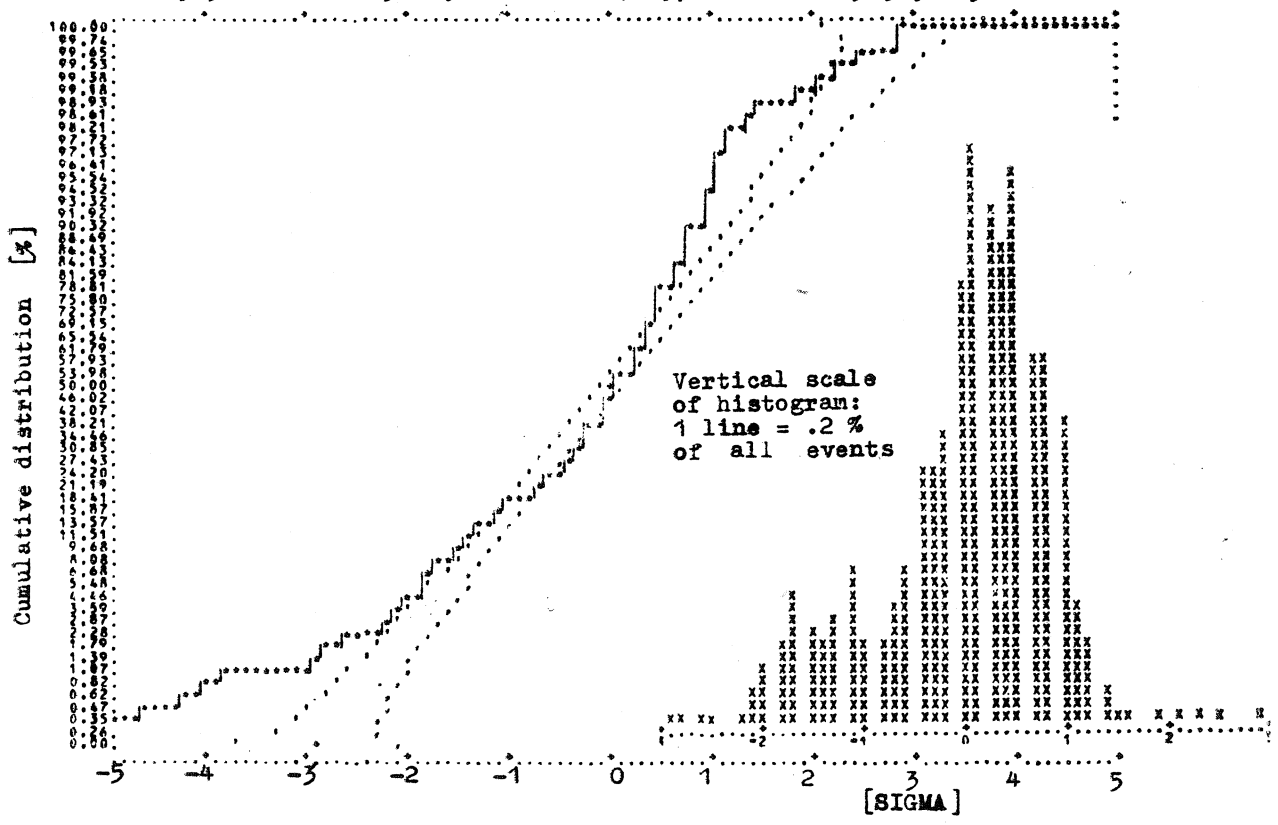

Fig. 8. Dry bulk density distribution for the sandstones from the whole Gorlice—Brzozów region

Fig. 8. Rozkład ciężaru objętościowego szkieletu dla piaskowców całego rejonu Gorlice—Brzozów. Pionowa skala histogramu: 1 linia = 0,2% wszystkich przypadków

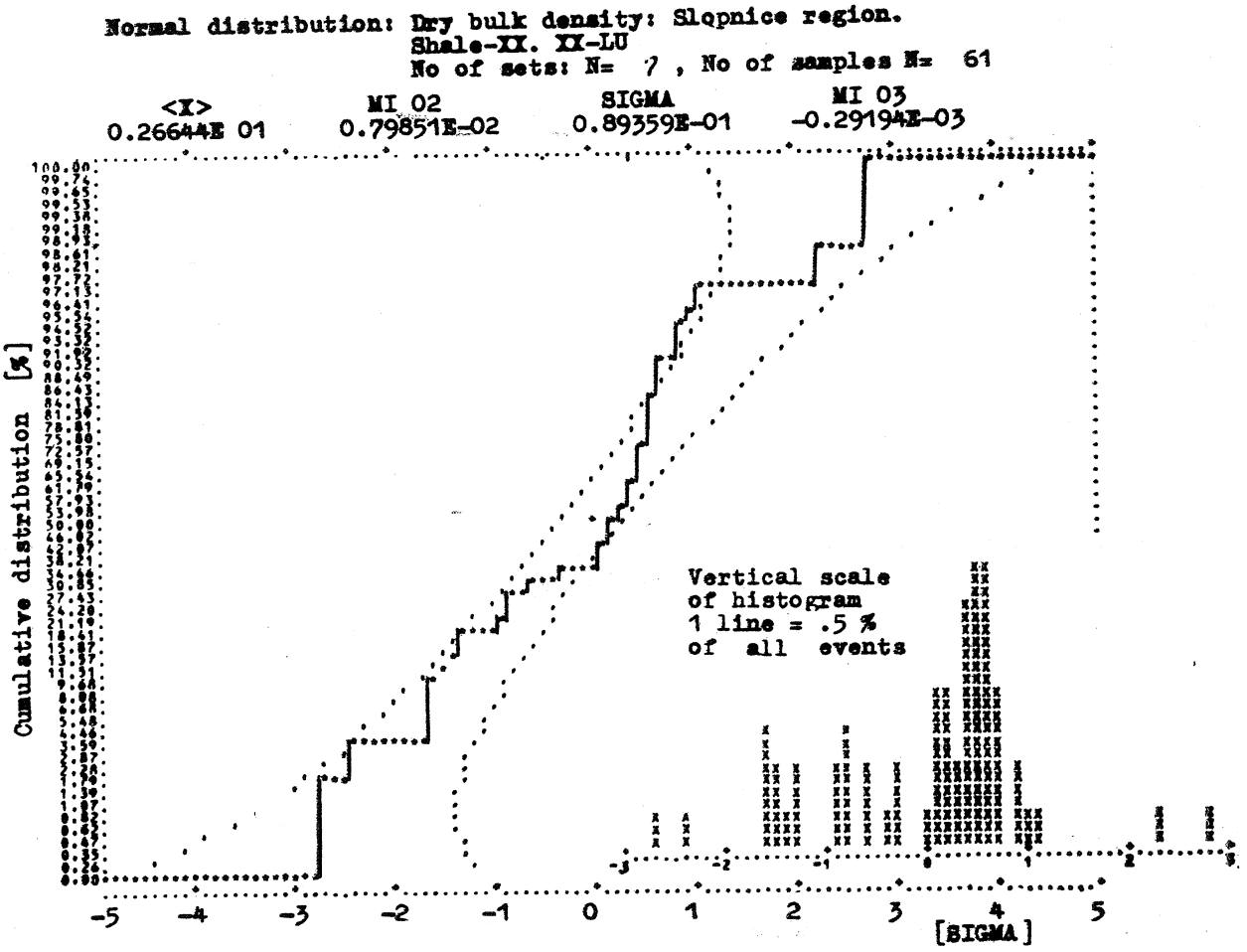

Fig. 10. Dry bulk density distribution for the shales from the Słopnice region

Fig. 10. Rozkład ciężaru objętościowego szkieletu dla łupków z rejonu Słopnic

Fig. 9. Dry bulk density distribution for the core samples taken from the Słopnice region

Fig. 9. Rozkład ciężaru objętościowego szkieletu dla próbek rdzeni wziętych z rejonu Słopnic. Pionowa skala histogramu: 1 linia = 0,2% wszystkich przypadków

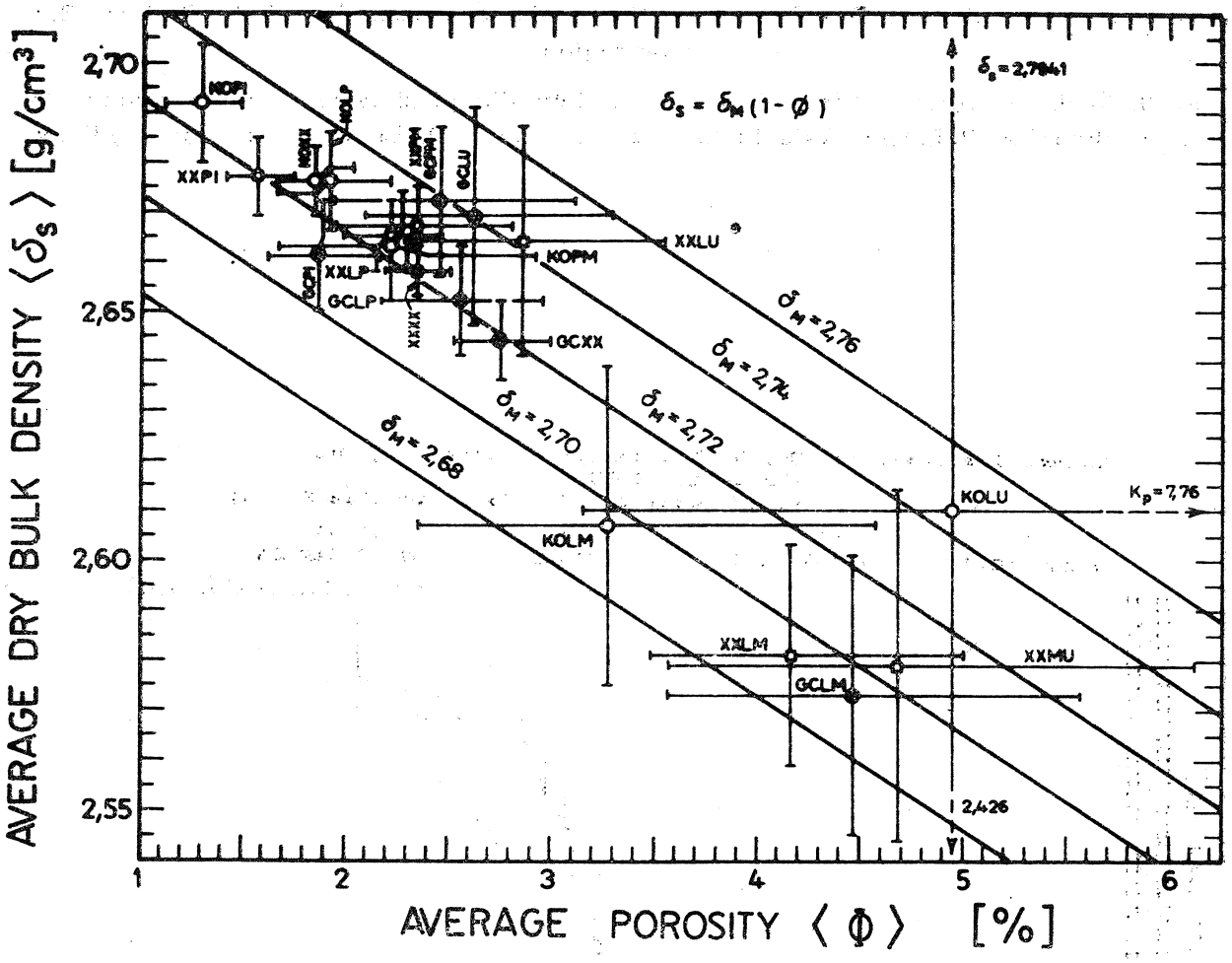

Fig. 11. Correlation between the expected values of dry bulk density and porosity for the Słopnice region

Fig. 11. Korelacja pomiędzy wartościami oczekiwanymi ciężaru objętościowego szkieletu i współczynnika porowatości dla rejonu Słopnic

clay minerals as being 2.65, 2.71 and δ_{sh} (unknown), respectively, it was easy to obtain that for the Słopnice region $\delta_{sh} = 2.80$ g/cm³ with the average (quarz + feldspar + carbonates) rock matrix mineralogical density $\delta_M = 2.67$ g/ccm. For the Potok Fold, by the same manner, it was obtained $\delta_{sh} = 2.65$ g/cm³. It should be noted here that when one wants to get these data from the direct correlation between the δ_s and Ø data for each sample, the result is not so clear. The examples are given in Figs 14 and 15. Here the δ_s vs Ø crosspiots are given for the Słopnice and for the Gorlice-Brzozów regions together with the regression lines. One can obtain, by the simple overlay of Eq. (2.1) onto these crossplots, the apparent densities $\tilde{\delta}_M$ equal to 3.4 or 2.2 g/cm³ which is, of course, not admissible for this kind of lithology. This effect is probably due to the low accuracy and/or confidence which can be paid to the laboratory data obtained from the core samples. Our approach based on the expected values of the marginal distributions for the joint distribution of these data is much more convenient, and the eventual inaccuracies in the

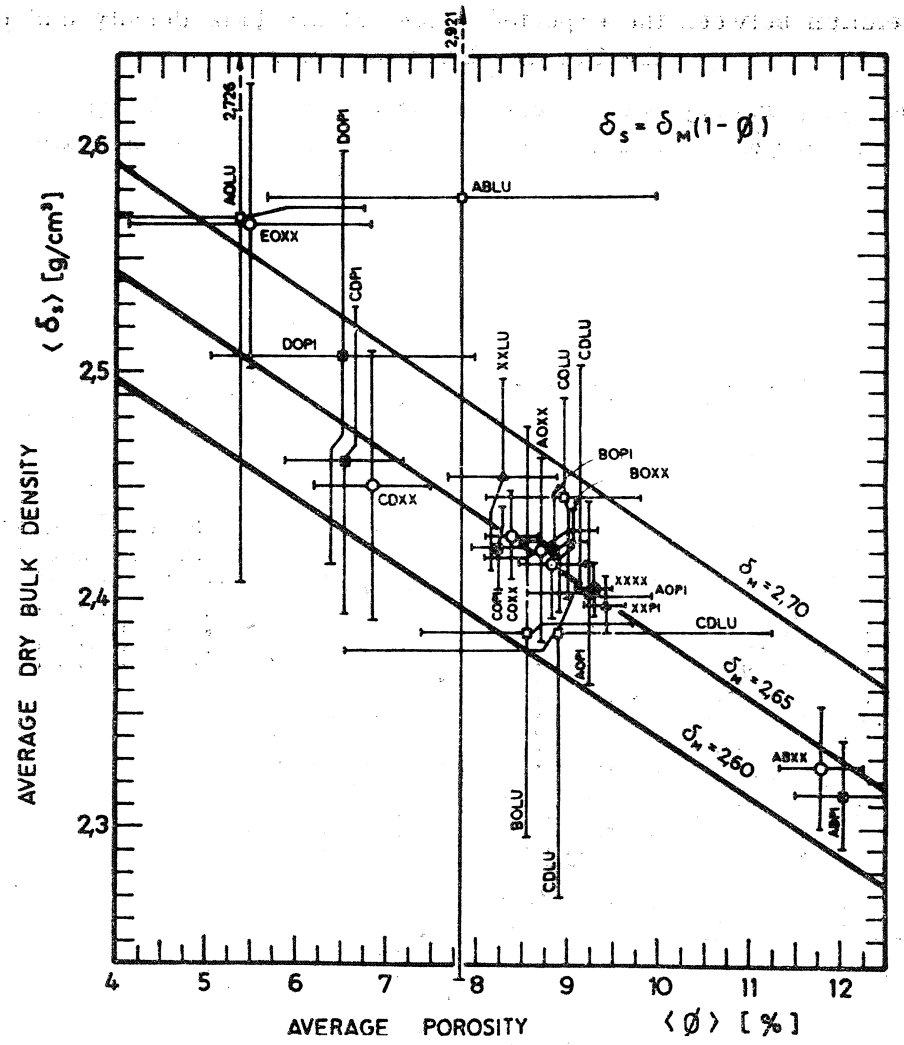
$\delta_s = \delta_M(1-\phi)$
AVERAGE DRY BULK DENSITY $\langle \delta_s \rangle$ [g/cm³]
AVERAGE POROSITY $\langle \phi \rangle$ [%]
2,6
2,5
2,4
2,3
4
5
6
7
8
9
10
11
12
2,921
2,726
δ_M = 2,70
δ_M = 2,65
δ_M = 2,60
ABLU
EOXX
DOPI
CDPI
COXX
XXLU
COLU
CDLU
AOXX
BOPI
BOXX
XXXX
AOPI
XXPI
ASXX
BOLU

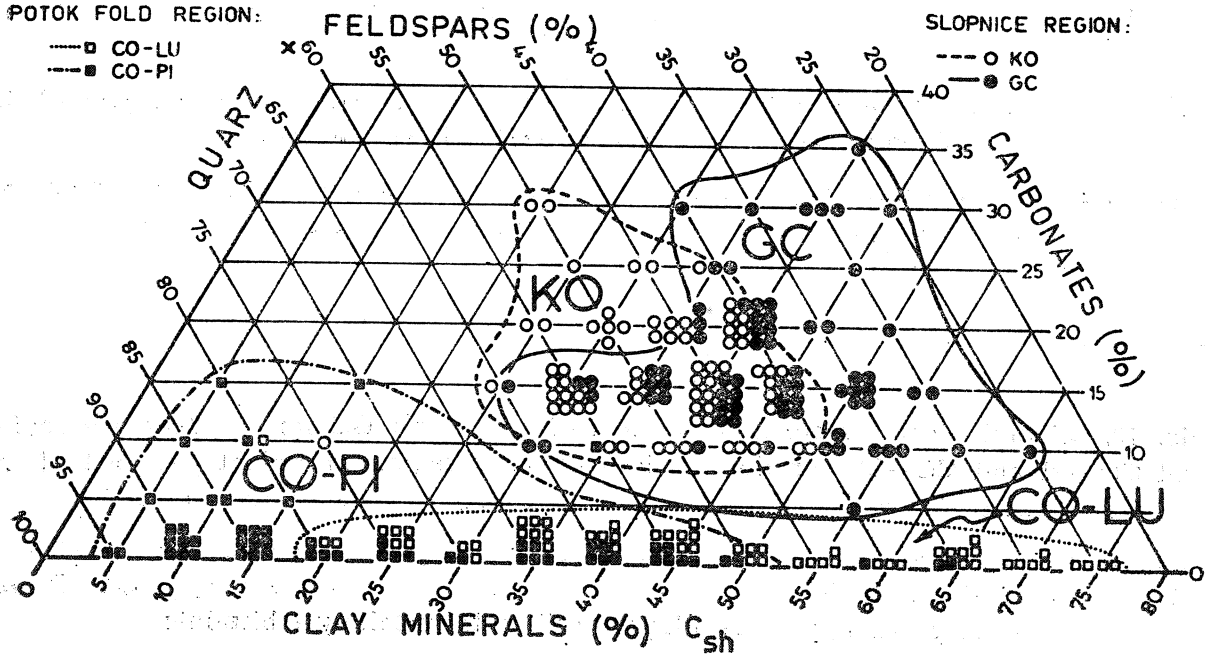
POTOK FOLD REGION:
CO-LU
CO-PI
SLOPNICE REGION:
KO
GC
FELDSPARS (%)
QUARZ
CARBONATES (%)
CLAY MINERALS (%) C_{sh}
CO-PI
KO
GC
CO-LU

Fig. 12. Correlation between the expected values of dry bulk density and porosity for the Gorlice—Brzozów region

Fig. 12. Korelacja pomiędzy wartościami oczekiwanymi ciężaru objętościowego szkieletu i współczynnika porowatości dla rejonu Gorlice—Brzozów

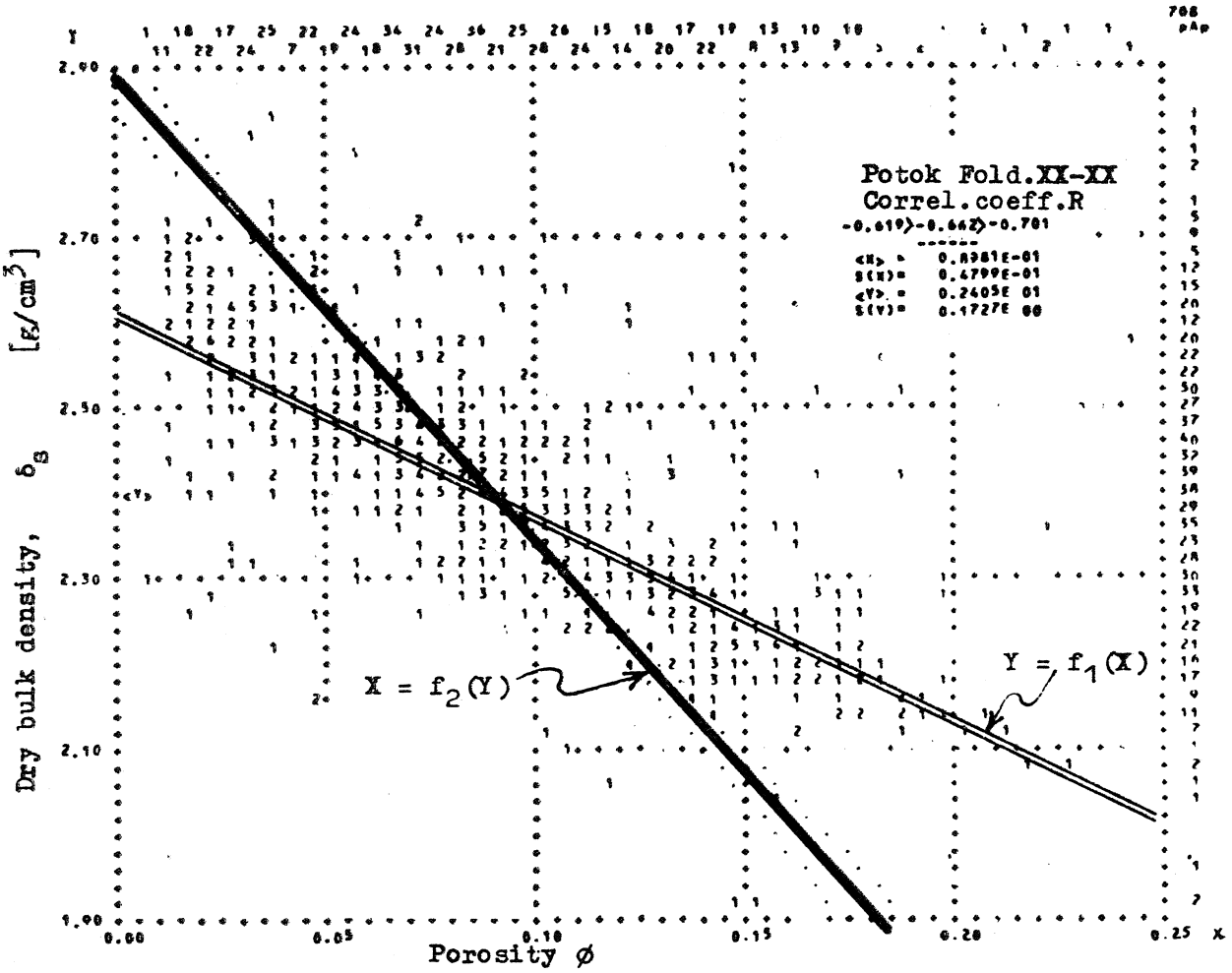

Fig. 14. Correlation between thy dry bulk density and porosity for the samples of the Słopnice region. The two regression lines are drawn

Fig. 14. Korelacja pomiędzy ciężarem objętościowym szkieletu a współczynnikiem porowatości dla próbek z rejonu Słopnic. Zaznaczono obie linie regresji

Fig. 13. Mineralogical composition of the series KO and GC for the Słopnice region and CO—PI and CO—LU for the Gorlice—Brzozów region in weight per cent of the dry sample. The range of occurrence for each series was defined arbitrarily

Fig. 13. Skład mineralogiczny serii KO i GC dla rejonu Słopnic oraz serii CO—PI i CO—LU dla rejonu Gorlice—Brzozów w procentach wagowych suchej próbki. Zasięg występowania poszczególnych serii został ustalony arbitralnie

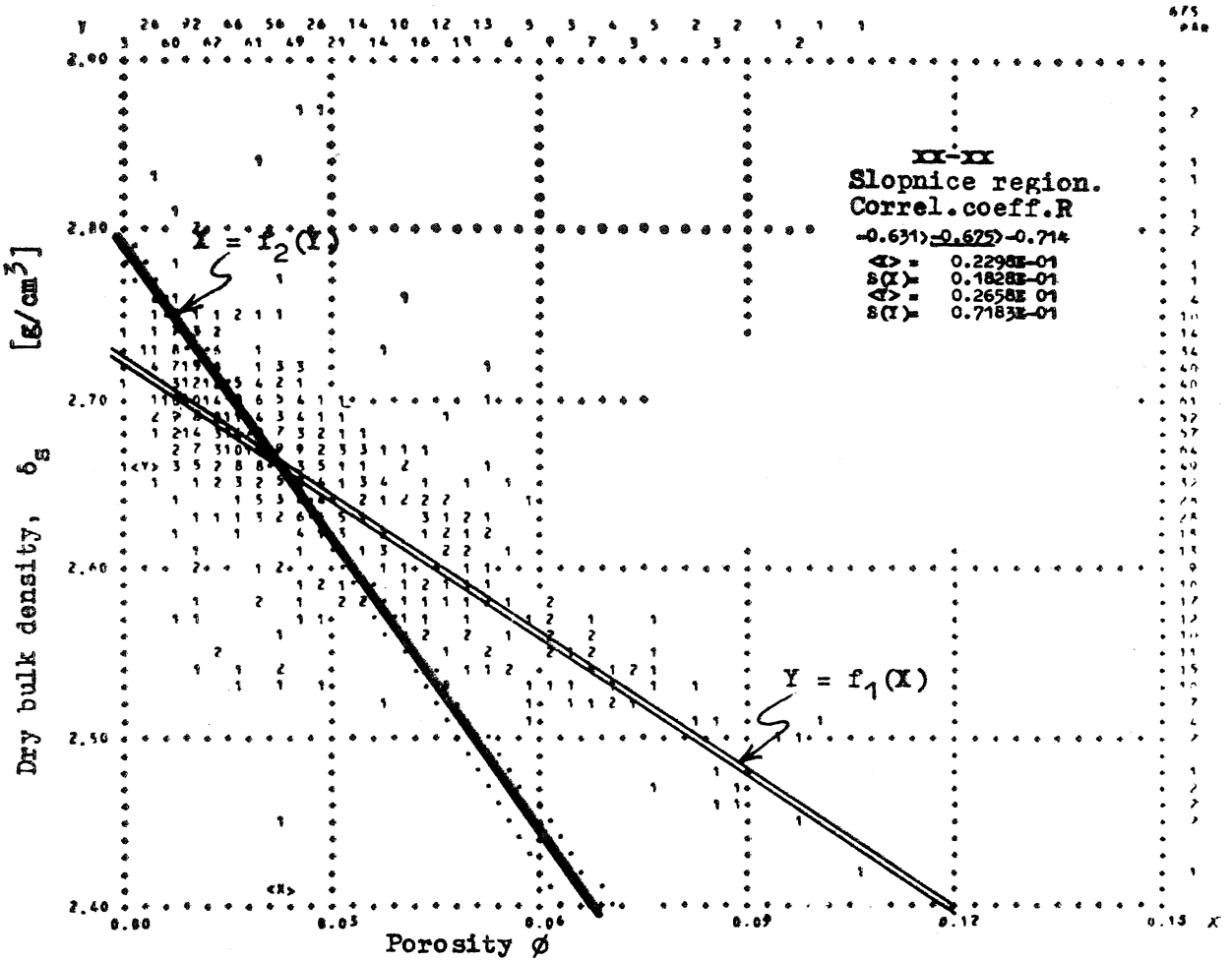

Fig. 15. Correlation between the dry bulk density and porosity for the samples of the **Gorlice—Brzozów region. The two regression lines are drawn**

Fig. 15. Korelacja pomiędzy ciężarem objętościowym szkieletu i współczynnikiem porowatości dla próbek rejonu Gorlice—Brzozów. Zaznaczono obie linie regresji

analysis results are increasing the confidence belts only. When the heterogenesity of the core samples is the cause of these discrepancy, our method eliminates it even completely.

CLAY CONTENT

The statistics for the clay C_{sh} (per weight) determinations was very poor for both regions (cf. Table 1.1.). Probably for this reason they follow rather well the normal distributions (within the 95 per cent confidence belt valid for this number of data!). An example of these distributions is given in Figs 16 and 17.

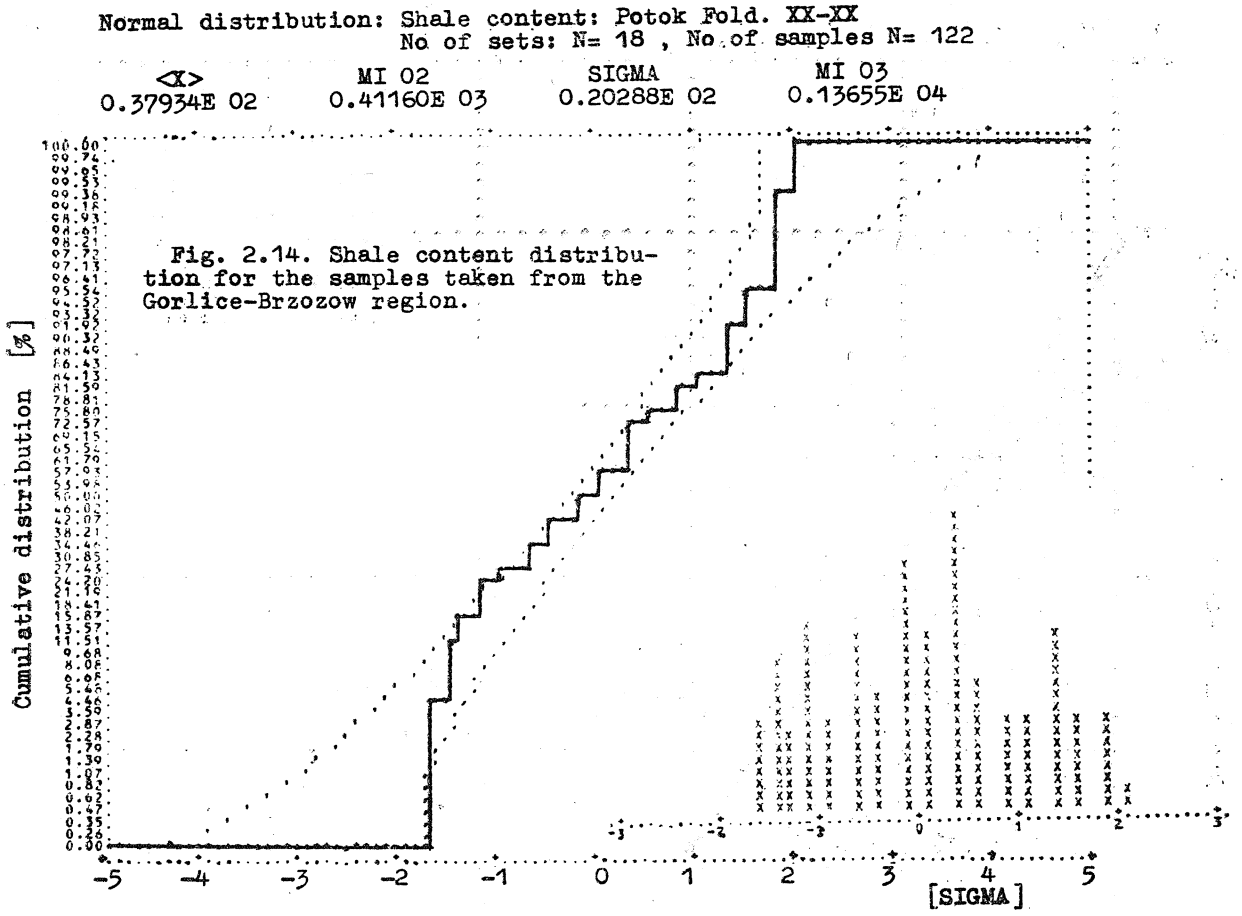

Fig. 2.14. Shale content distribution for the samples taken from the Gorlice-Brzozow region.

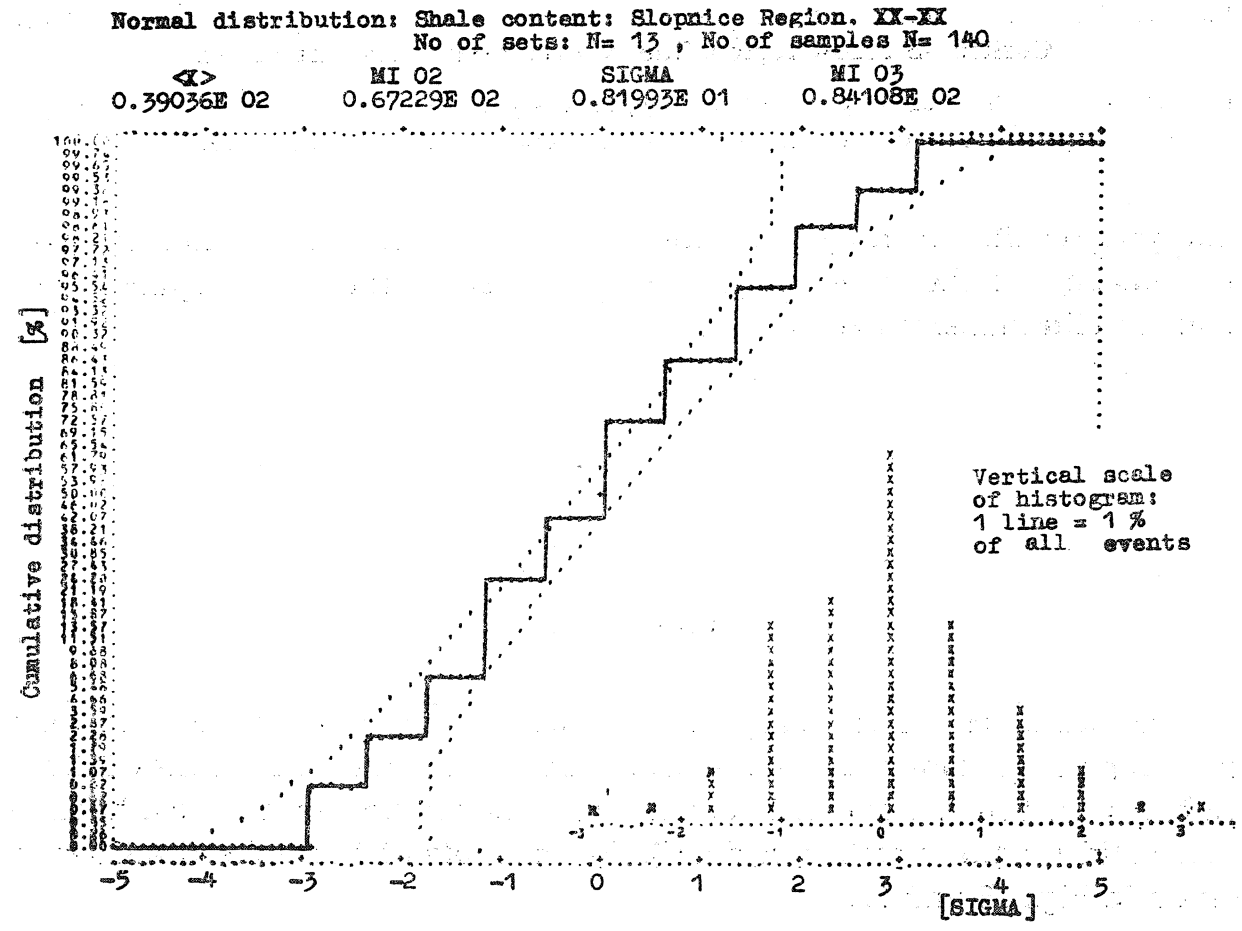

Fig. 16. Shale content distribution for the samples taken from the Gorlice—Brzozów region

Fig. 16. Rozkład zawartości iłu w próbkach wziętych z rejonu Gorlice—Brzozów. Pionowa skala histogramu: 1 linia = 0.5% wszystkich przypadków

PERMEABILITY

We have performed the correlation between the porosity and the logarithm of the permeability for the core sample data obtained for the Gorlice-Brzozów region. An example for such correlation is given in Fig. 18 for the sandstones of the C series in the Potok Fold. This correlation is rather poor but significant. A very similar picture was obtained for the other litho-stratigraphic series in this region.

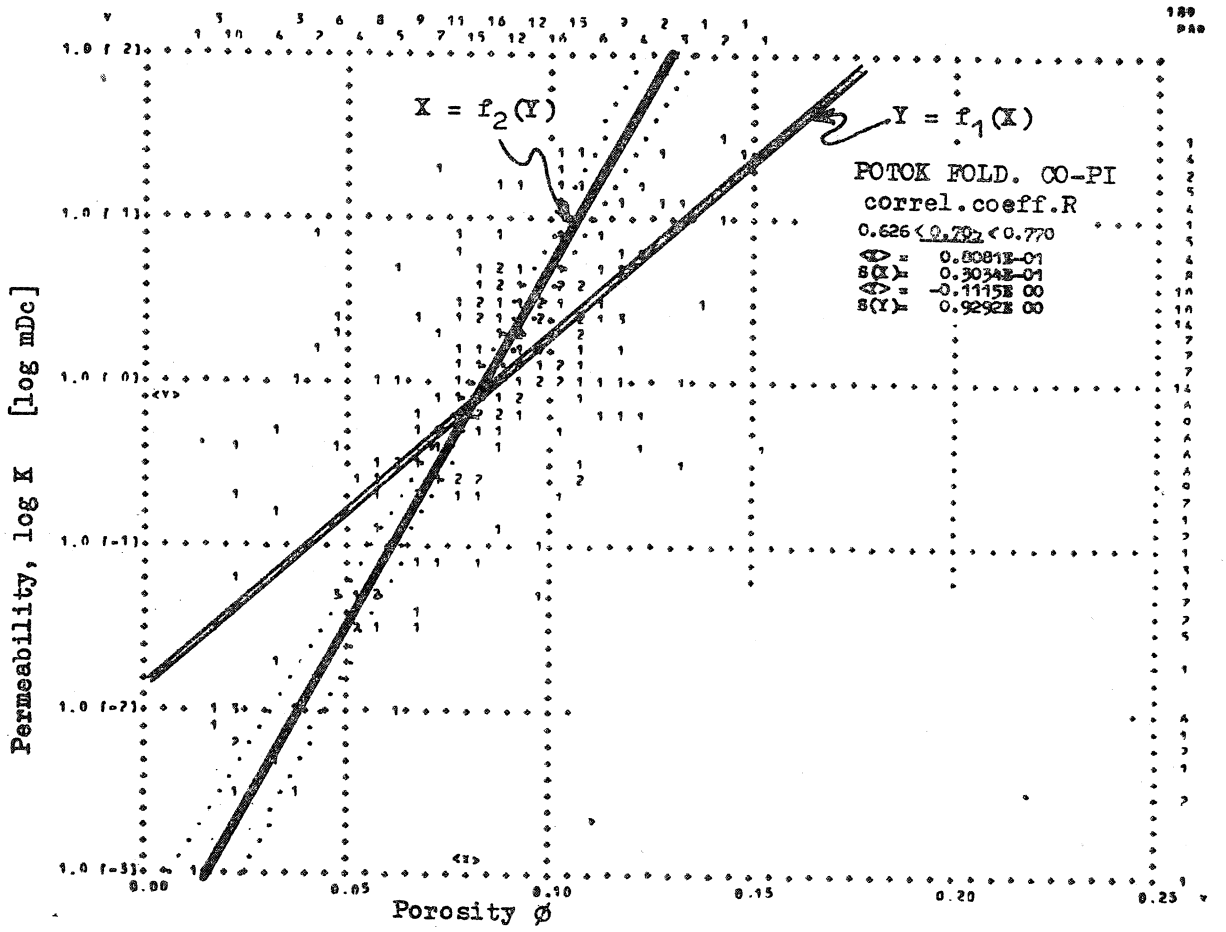

Fig. 18. Correlation between the porosity and the logarithm of the permeability for the samples of the sandstone C in the Potok Fold. The two regression lines are drawn
Fig. 18. Korelacja pomiędzy współczynnikiem porowatości a logarytmem współczynnika przepuszczalności dla próbek piaskowców C Fałdu Potoka. Zaznaczono obie linie regresji

Fig. 17. Shale content distribution for the samples taken from the Słopnice region

Fig. 17. Rozkład zawartości iłu w próbkach wziętych z rejonu Słopnic. Pionowa skala histogramu: 1 linia = 1% wszystkich przypadków

VARIOGRAMS

The variograms $\gamma(d)$ (Matheron, 1965) of the porosity and of the bulk density have been calculated. Because of the well-to-well shortest distance of the order of about 1 km, the vertical variograms had some acceptable behaviour only. We have calculated them as the average for all boreholes in a given region, excluding from the computation some layers for which we already knew (from the previous calculations) their strange behaviour.

In the Slopnice region the porosity Ø followed more or less the de Wijs scheme:

$$\gamma(d) = 3.\alpha.[\ln(d/l) + 3/2] \tag{2.2}$$

with $\alpha = 8.10^{-6}$ [%² · 10^{-4}] and $l = 7$ cm,

whereas for the Gorlice-Brzozów region this variogram was of the spherical type:

$$\gamma(d) = C \cdot \begin{cases} (3/2) \cdot (d/a) - (1/2) \cdot (d/a)^3 & d \leqq a \\ 1 & d \geqq a \end{cases} \tag{2.3}$$

with $C = 1.5\ 10^{-3}$ [%² · 10^{-4}] and $a = 1.5$ m.

The examples of these variograms are given in Figs 19 and 20, where for the variograms given by Eqs (2.2) and (2.3) the confidence belts of

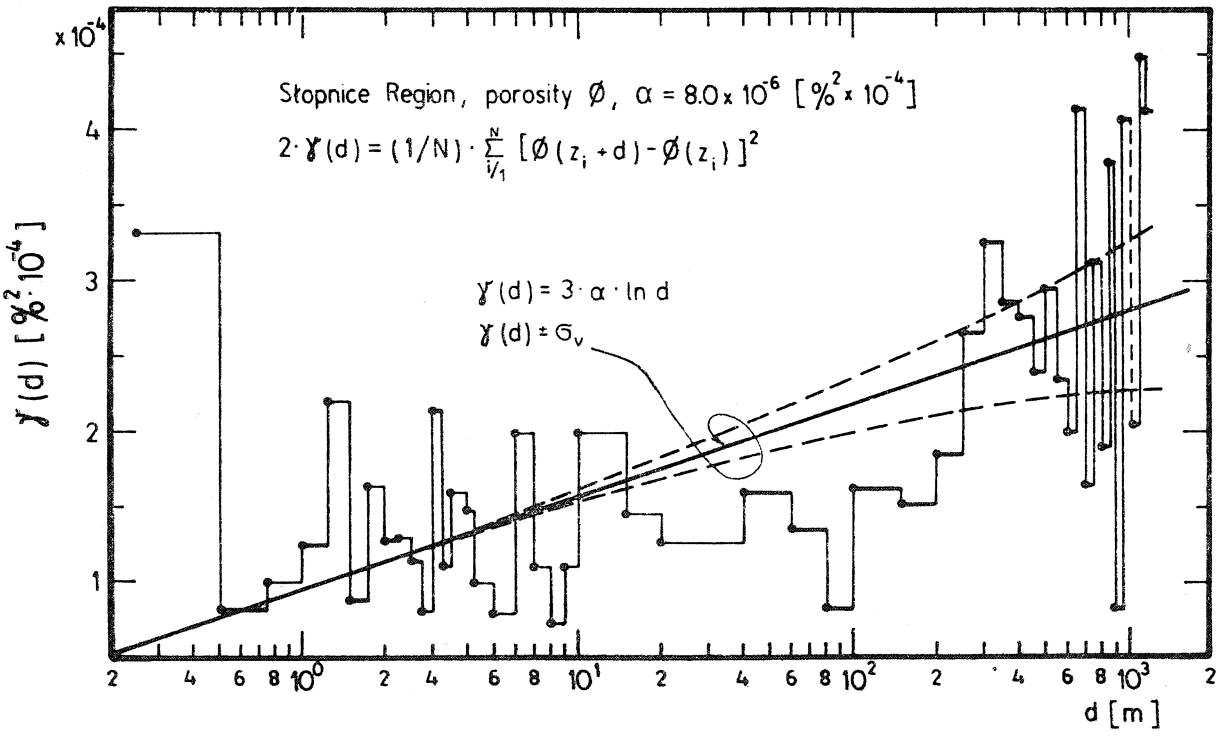

Fig. 19. Vertical variogram of porosity for the Słopnice region. The experimental data marked by heavy points (●) have been obtained from less than 50 pairs of data

Fig. 19. Pionowy wariogram współczynnika porowatości dla rejonu Słopnice. Dane doświadczalne zaznaczono pełnymi kółkami (●) zostały otrzymane z mniej niż 50 par danych

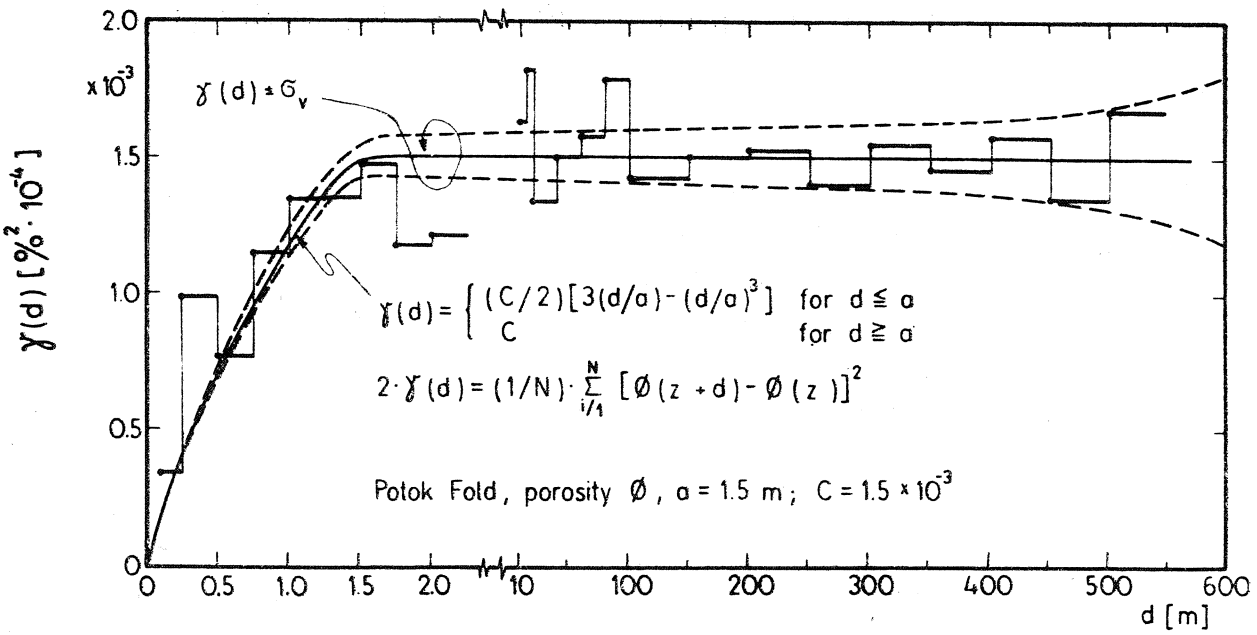

Fig. 20. Vertical variogram of porosity for the Gorlice—Brzozów region. Porosity data are taken from the core samples

Fig. 20. Pionowy wariogram współczynnika porowatości dla rejonu Gorlice—Brzozów. Współczynnik porowatości był mierzony na próbkach rdzeni

$\pm\ \sigma_v$ have been calculated. The standard deviation σ_v has been obtained as the fluctuations of the so called local variogram according to the Matheron's idea (Matheron, 1965).

The variograms for the δ_s values have been of the de Wijs type for both regions with the α coefficients of the order of 1.1 10^{-4} g²/cm⁶ for the Słopnice region, and $\alpha = 6.5\ 10^{-4}$ g²/cm⁶ for the other one, but the agreement with the experimental variograms was rather poor one.

The spherical variograms of the porosity shown in Fig. 10 has been used to recalculate the porosity variance "seen" by the borehole neutron tool. Here the knowledge of the function F(v) in the three dimensional space was needed for the spherical variogram (Matheron, 1965)

$$F(v) = \frac{1}{v^2} \int_v \int_v \gamma(\vec{x}-\vec{x}').d\vec{x}.\vec{x}', \tag{2.4}$$

where v is the volume of the sample, the elementary volumes $d\vec{x}$ and $d\vec{x}'$ are located at the two extermities of the vector $\vec{h}=\vec{x}-\vec{x}'$ and they are walking independently each other inside the volume v. This sextuple integral can be reduced to the triple one which in the case of the variogram of the type h^λ and for the rectangular parallelepiped (for the volume v) of the dimensions $\tilde{a} \geqq b \geqq c$ is of the form:

$$F_\lambda(\tilde{a},b,c) =$$

$$= \frac{8}{\tilde{a}^2b^2c^2} \int_0^{\tilde{a}} \int_0^{b} \int_0^{c} (a-x).(b-y).(c-z).(x^2+y^2+z^2)^{\lambda/2}.dx.dy.dz \tag{2.5}$$

which for the spherical variogram given by Eq. (2.3) finally gives:

$$\frac{F_{sph}(\tilde{a},t)}{C} =$$

$$= \tilde{a}.[0.5 - t^2.(0.5\ \ln t - 2.8556905 \cdot 10^{-1}) +$$
$$t^3 \cdot 2.4072624 \cdot 10^{-1} - t^4 \cdot 3.54166 \cdot 10^{-2} +$$
$$t^6 \cdot 2.1577381 \cdot 10^{-3} - t^8 \cdot 4.6378412 \cdot 10^{-4} + ...] -$$
$$\tilde{a}^3 \cdot [0.05 + t^2 \cdot 8.333317 \cdot 10^{-2} + t^4 \cdot (4.6203835 \cdot 10^{-2} -$$
$$7.083333 \cdot 10^{-2} \cdot \ln t) + t^5 \cdot 3.1561269 \cdot 10^{-2} -$$
$$t^6 \cdot 4.3154739 \cdot 10^{-3} + t^8 \cdot 2.3189507 \cdot 10^{-4} - ...], \qquad (2.6)$$

where $b = c$

$$t = b/\tilde{a} \leqq \sqrt{0.5\,(\tilde{a}^{-2} - 1)} \qquad (2.7)$$

and the sizes of the parallelepiped are expressed in the units of the range a of the spherical variogram (cf. Eq. (2.3)), thus $\tilde{a} \leqq 1$. The plot of the function given by Eq. (2.6) is given in Fig. 21. The, so called, linear equivalents for the parallelepipeds in the spherical scheme can be obtained from these data.

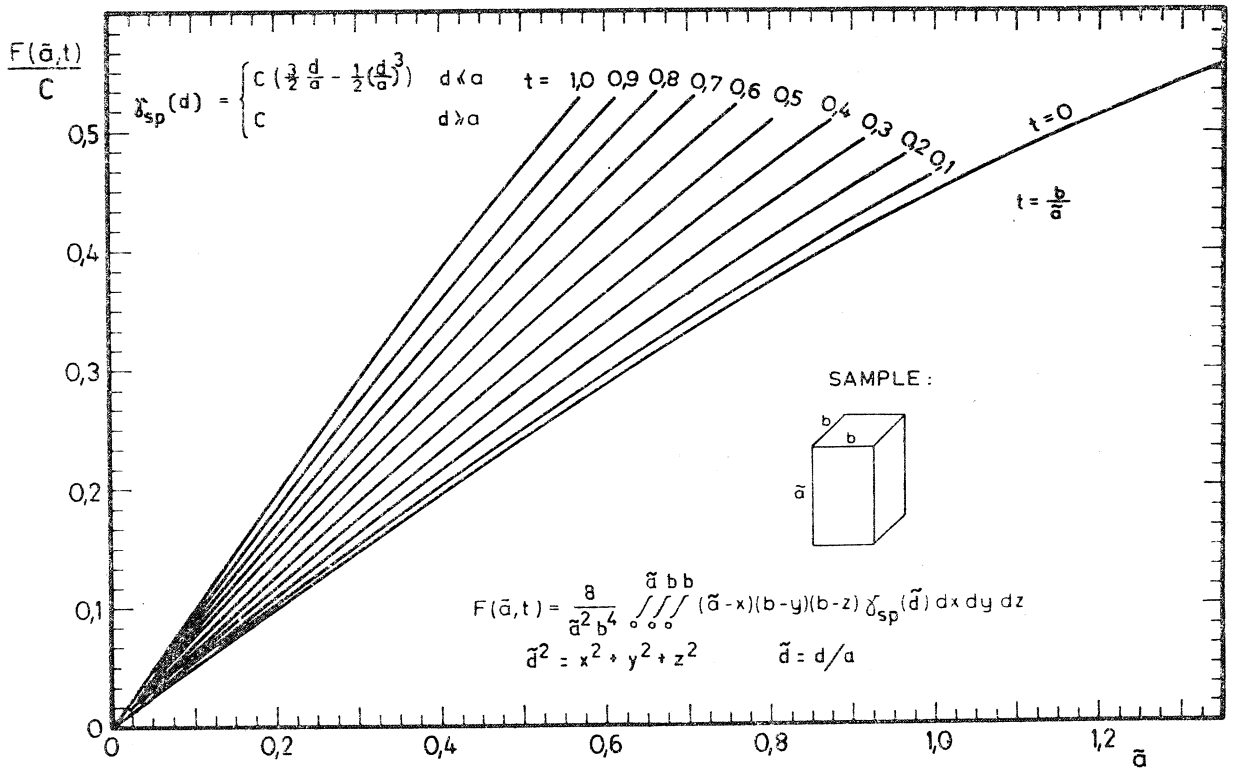

Fig. 21. Plot of the function $F_{sph}(\tilde{a}, t)$ for the spherical variogram, given by Eq. (2.6). The sizes of the parallelepiped are in the units of the range a of the spherical variogram

Fig. 21. Wykres funkcji $F_{sph}(\tilde{a}, t)$ dla wariogramu sferycznego wg wzoru (2.6). Rozmiary prostopadłościanu są podobne w jednostkach zasięgu a wariogramu sferycznego

3. LOGGING DATA TREATMENT

Using the deterministic approach (Zorski, 1979, Czubek and Zorski, 1979) the gamma-ray and the neutron-gamma ray logging data were recalculated to obtain the logging deflections free of the influence of the apparatus and of the borehole conditions.

The crossplot of the neutron and gamma-ray logging deflections give and information about the lithology in the shaly-sandstone sequence, as it is shown in Fig. 22.

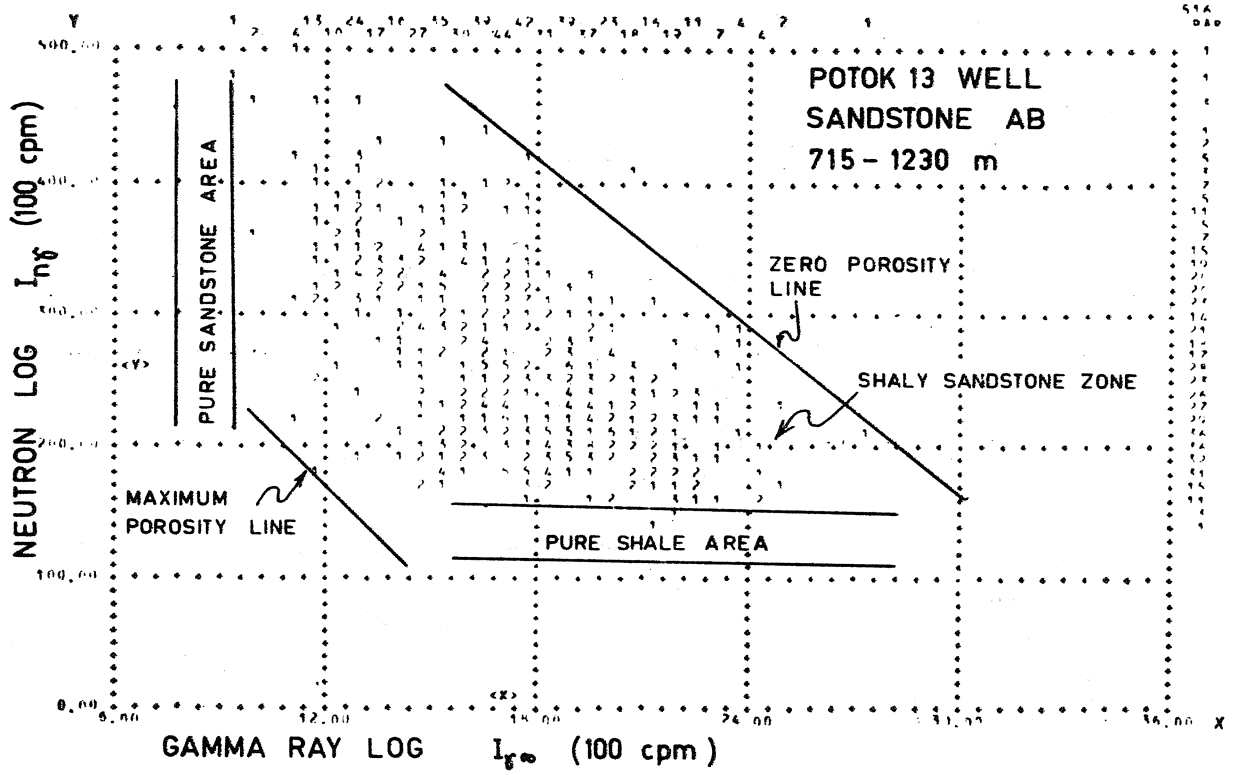

Fig. 22. Crossplot of the neutron and gamma-ray log deflections for sandstones in the Potok 13 borehole. The lithology identification zones deliminate this part of the borehole as the shaly sandstone of different porosity

Fig. 22. Zestawienie wskazań profilowań neutronowych i gamma dla piaskowców Otworu Potok-13. Strefy identyfikacji litologicznej określają tę część otworu jako zailany piaskowiec o zmiennym współczynniku porowatości

The variograms of the $I_{\gamma\infty}$ (natural radioactivity) and $I_{n\gamma}$ (neutron-gamma log deflections) intensities give the information about the variograms of the shale content and that of the porosity. An example is shown in Figs 23 and 24 for the sandstone of the B series in the Sobniów 23 borehole (Potok Fold).

An interesting information can be obtained from the correlation between the gamma-ray and the neutron-gamma variograms for a given formation. Such correlation for the sandstone of the C series in the Sobniów 23 borehole is given in Fig. 25. Here, for the distance d lower than

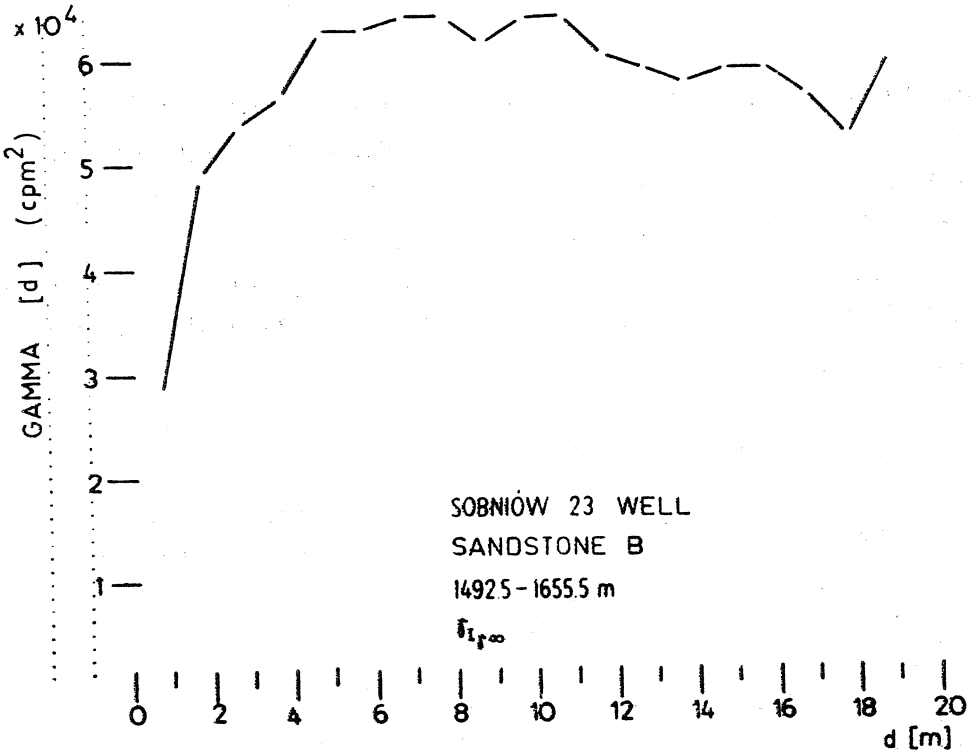

Fig. 23. Variogram of the natural radioactivity for the sandstones of the B series in the Sobniów 23 borehole

Fig. 23. Wariogram naturalnej promieniotwórczości dla piaskowców serii B w otworze Sobniów 23

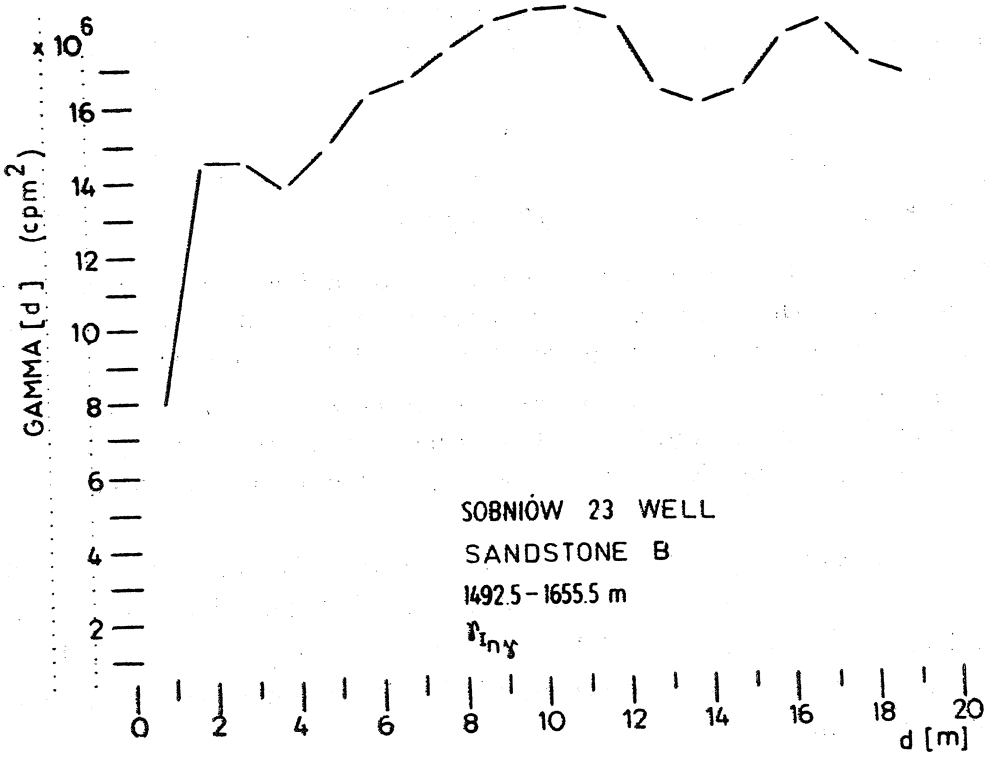

Fig. 24. Variogram of the neutron-gamma ray log deflections for the sandstones of the B series in the Sobniów 23 borehole taken for the same well section as in Fig. 23

Fig. 24. Wariogram wskazań profilowania neutron-gamma dla piaskowców serii B w otworze Sobniów 23 wziętych dla tego samego odcinka otworu jak na Fig. 23

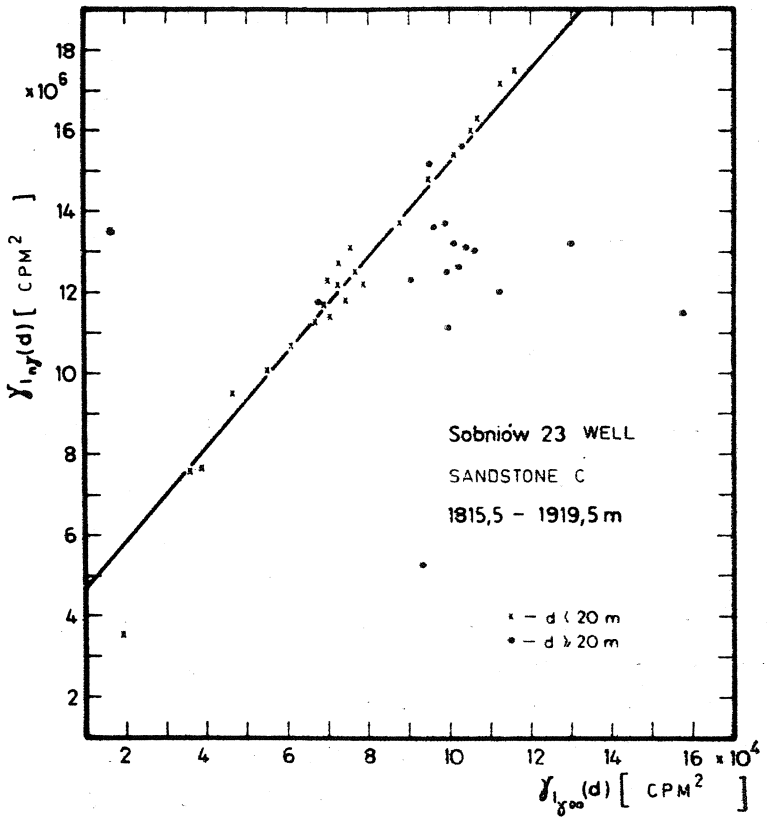

Fig. 25. Correlation between the $\gamma_{I_{\gamma\infty}}(d)$ and $\gamma_{I_{n_\gamma}}(d)$ variograms. This correlation has the physical meaning for the distances d lower than the range a of the spherical variogram. Here, for the logging data in the sandstones of the C series in the Sobniów 23 borehole, the range a has been estimated as a = 20 m

Fig. 25 Korelacja pomiędzy wariogramami $\gamma_{I_{\gamma\infty}}(d)$ i $\gamma_{I_{n_\gamma}}(d)$. Ta korelacja ma fizyczny sens dla odległości d mniejszych niż zasięg a wariogramu sferycznego. Tutaj, dla piaskowców serii C w otworze Sobniów 23 zasięg wariogramu dla wyników profilowań został określony na a = 20 m

the range a = 20 m of the spherical variograms $\gamma_{I_{\gamma\infty}}(d)$ and $\gamma_{I_{n\gamma}}(d)$, the linear relationship can be found:

$$\gamma_{I_{n\gamma}}(d) = B + S \cdot \gamma_{I_{\gamma\infty}}(d), \tag{3.1}$$

where the nature of the constants B and S is that:

$$B/S = 6.25 \cdot \sigma^2(\emptyset) \cdot K^2, \tag{3.2}$$

where $\sigma^2(\emptyset)$ is the variance of the porosity "seen" by the neutron probe, and K is the calibration factor for the gamma-ray log when the shale content C'_{sh} (per weight of the rock "in situ" is determined from this kind of log:

$$I_{\gamma\infty} = K_o + K \cdot C'_{sh} \ . \tag{3.3}$$

Using all this statistical and geostatistical information the statistical calibration curves (Bogacz et al., 1979, Czubek et al., 1977) have been found. Thus, the volume shale content V_{sh} and the rock porosity Ø from the gamma-ray and neutron-gamma ray logs have been obtained. Here

the three different shale contents have been carefully taken into account: C_{sh} — the shale content per weight of the dry rock, C'_{sh} — the shale content per weight of the natural, in situ rock (when the pore space fulfilment is also taken into account), and V_{sh} — the volume shale content. The first one is measured in the laboratory on the core samples, the second one by the gamma-ray log, whereas the third one influences the neutron log deflections.

4. TREATMENT OF THE LOG DERIVED PARAMETERS

From the quantitative interpretation of nuclear logs, using the statistical calibration curves, the shale content V_{sh} and the rock porosity Ø are obtained. These values can be treated again by the statistical and geostatistical ways. Here the statistical distributions of V_{sh} are very like those for the $I_{\gamma\infty}$ values. The log derived porosities Ø fit quite well the distributions still found from the core sample data analysis.

The variograms of the V_{sh} values show the same behaviour as the variograms of the $I_{\gamma\infty}$ data. The variogram of the log derived porosites Ø is

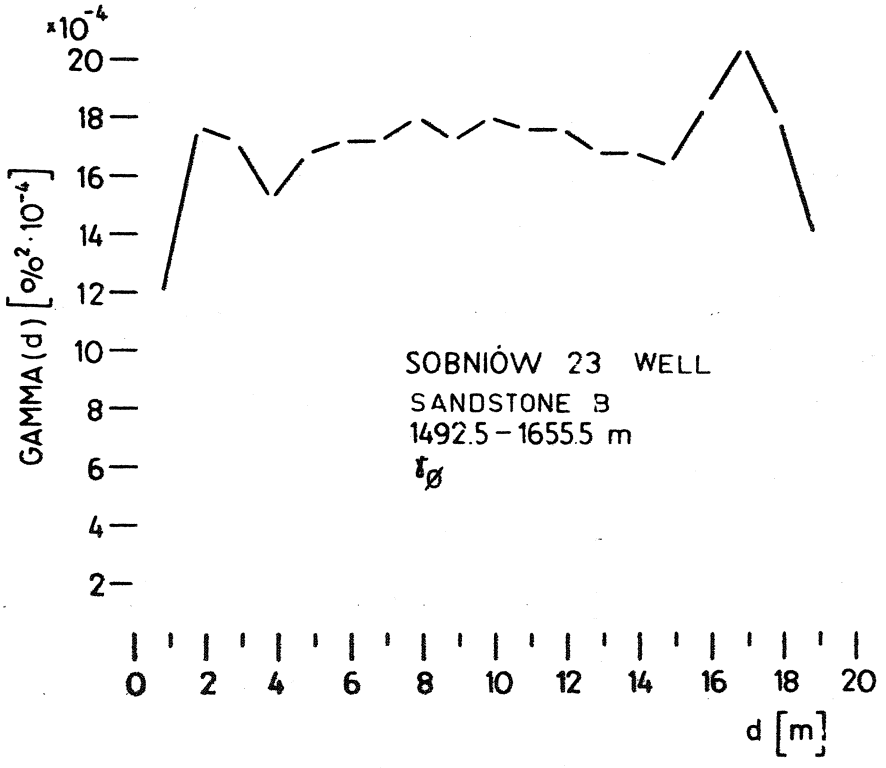

Fig. 26. Variogram of the log derived porosities for the sandstones of the B series in the Sobniów 23 borehole taken for the same well section as in Figs 23 and 24

Fig. 26. Wariogram dla współczynnika porowatości z interpretacji profilowań dla piaskowców serii B w otworze Sobniów 23 wzięty dla tego samego odcinka otworu jak na Fig. 23 i Fig. 24

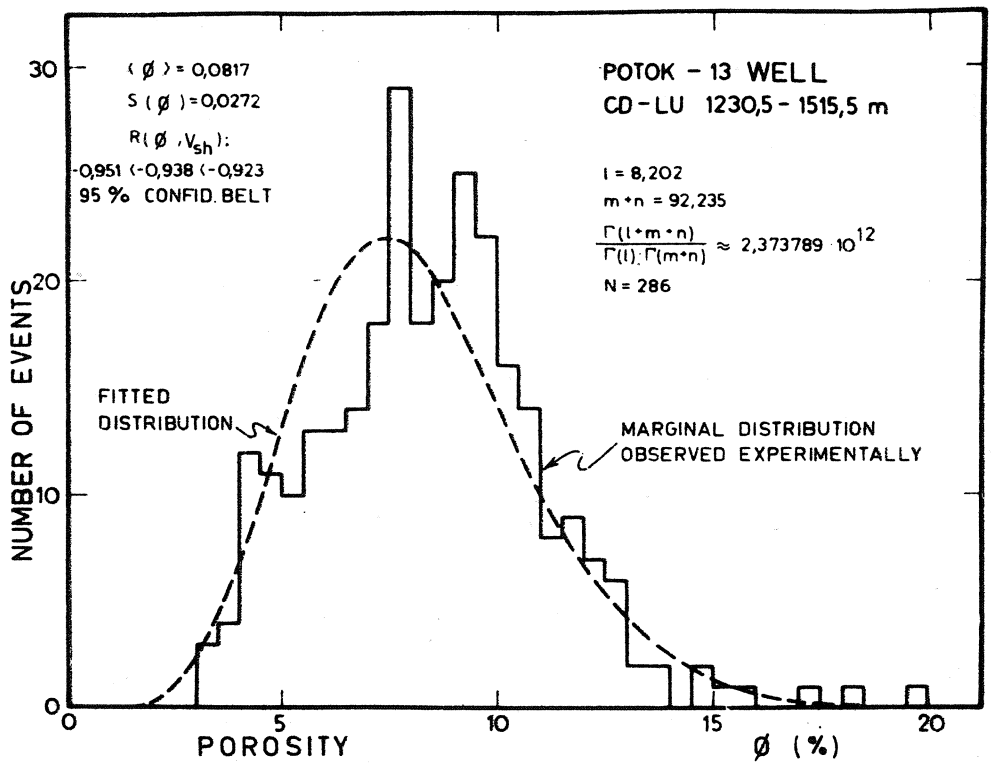

Fig. 27. Fit of the beta distribution to the experimentally observed marginal distribution of the log derived porosities

Fig. 27. Dopasowanie rozkładu beta do obserwowanego doświadczalnie rozkładu brzegowego współczynników porowatości otrzymanych z interpretacji profilowań

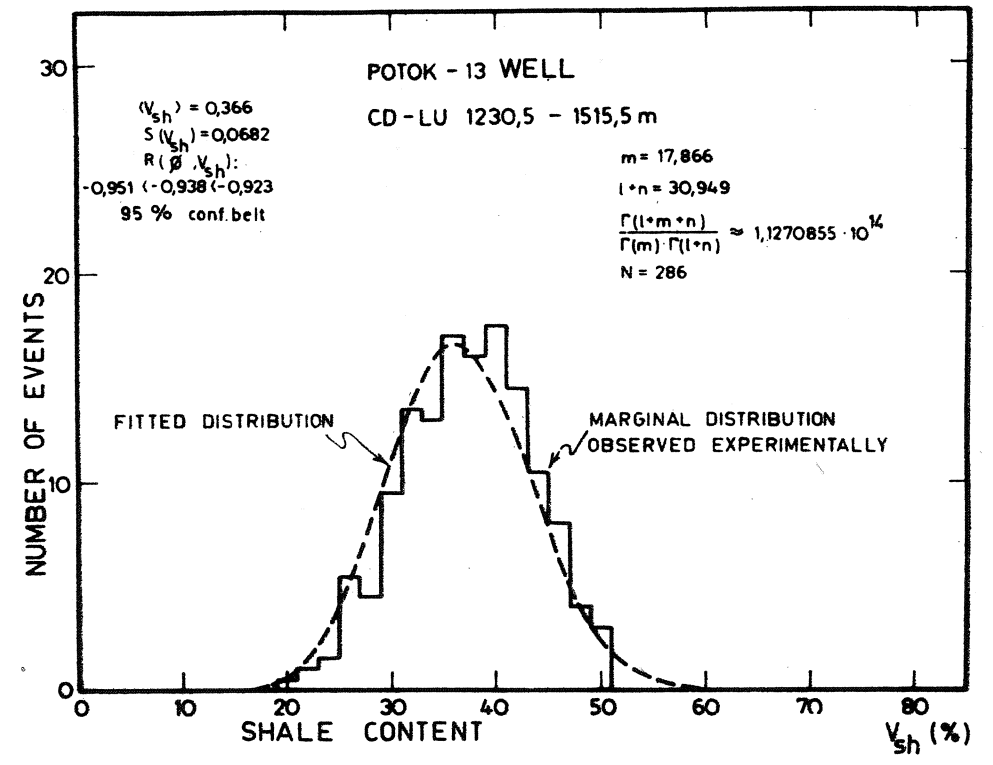

Fig. 28. Fit of the beta distribution to the experimentally observed marginal distribution of the log derived shale content

Fig. 28. Dopasowanie rozkładu beta do obserwowanego doświadczalnie rozkładu brzegowego zailenia otrzymanego z interpretacji profilowań

shown in Fig. 26 for the sandstones of the B series in the Sobniów 23 borehole. When one compares this variogram with the variogram of the $I_{n\gamma}$ values given in Fig. 24 for the same borehole section, the net difference is visible. The log derived porosity Ø has the spherical variogram (but regularized over the rock volume "seen" by the neutron tool) which is essentially similar to this one from Fig. 20 obtained for the core samples from this region.

Because all the variograms for the log derived shale content and porosity have the spherical shape, the obvious conclusion is that there is no vertical trend for these data, at least along the borehole sections investigated here

The crossplot of the log derived shale content with the porosity shows again a very distinct lithology effect. For the pure shale sections this correlation follows very well the straight line with the negative slope, whereas for the shaly sandstones the data are dispersed inside the triangle which sides are defined by the pure shale of different porosity, pure sandstone of different porosity and hard shaly sandstone.

When the normal distributions for the shale content V_{sh} and for the porosity Ø have been found, we have been quite conscious of the ambiguity of these results. Both parameters, being limited inside the [0;1] section, cannot follow exactly the normal distribution. Just in this case the beta distribution of the first kind seems to be more appropriate. Thus, we have tried, starting from the assumption that both V_{sh} and Ø follow the joined bivariate beta distribution (within the given litho-stratigraphic series), to find the parameters of these distributions. These parameters have been derived from the marginal distributions of the V_{sh} and that of Ø. These marginal distributions should also be of the beta kind, and really, they are. An example is given in Figs 27 and 28, but their parameters do not fit the same bivariate beta distribution (compare, for example, the sum of (l + m + n) on both figures) which should have the form:

$$b(Ø,V_{sh} \mid l,m,n) = \frac{\Gamma(l+m+n)}{\Gamma(l)\cdot\Gamma(m)\cdot\Gamma(n)} \cdot Ø^{l-1} \cdot V_{sh}{}^{m-1} \cdot (1 - Ø - V_{sh})^{n-1}. \quad (4.1)$$

For such distribution the correlation coefficient ϱ between the Ø and V_{sh} variables is given as:

$$\varrho(Ø,V_{sh}) = -\sqrt{\frac{l\cdot m}{(n+l)\cdot(m+n)}} = \quad (4.2.a)$$

$$= -\sqrt{\frac{\langle Ø\rangle \cdot \langle V_{sh}\rangle}{(1-\langle Ø\rangle)\cdot(1-\langle V_{sh}\rangle)}}, \quad (4.2.b)$$

where $\langle Ø\rangle$ and $\langle V_{sh}\rangle$ correspond to the expected values. Thus, the correlation coefficient $\varrho(Ø,V_{sh})$ is always negative for the bivariate beta distribution.

Is really the rock porosity Ø correlated with its shale content V_{sh}? Here we have to distinguish the two different kinds of correlations. One is the intrinsic one connected with the sedimentation phenomena (correlation between the amount of the sand and that of the shale material transported to the deposition area), and the second one which is the spurious one, connected with the definition of Ø and that of V_{sh} which both, together with the rock matrix volume V_M, give always the sum equal to 1. Thus, the correlation between the rock porosity and its shale content is the problem of the ratio correlation (Chayes, 1971) In the case of the bivariate beta distribution the correlation coefficient given by Eq. (4.2) is known as the one obtained when the intrinsic correlation between the physical phenomena of porosity and that of the shale content does not exist. Basing on these considerations we have calculated the correlation coefficients ϱ according to Eq. (4.2.b) and the "usual" correlation coefficient R:

$$R = \frac{\sum_{j=1}^{n} (Ø_j - \langle Ø \rangle) \cdot (V_{sh_j} - \langle V_{sh} \rangle)}{\sqrt{\sum_{j=1}^{n} (Ø_j - \langle Ø \rangle)^2 \cdot \sum_{j=1}^{n} (V_{sh_j} - \langle V_{sh} \rangle)^2}} \qquad (4.3)$$

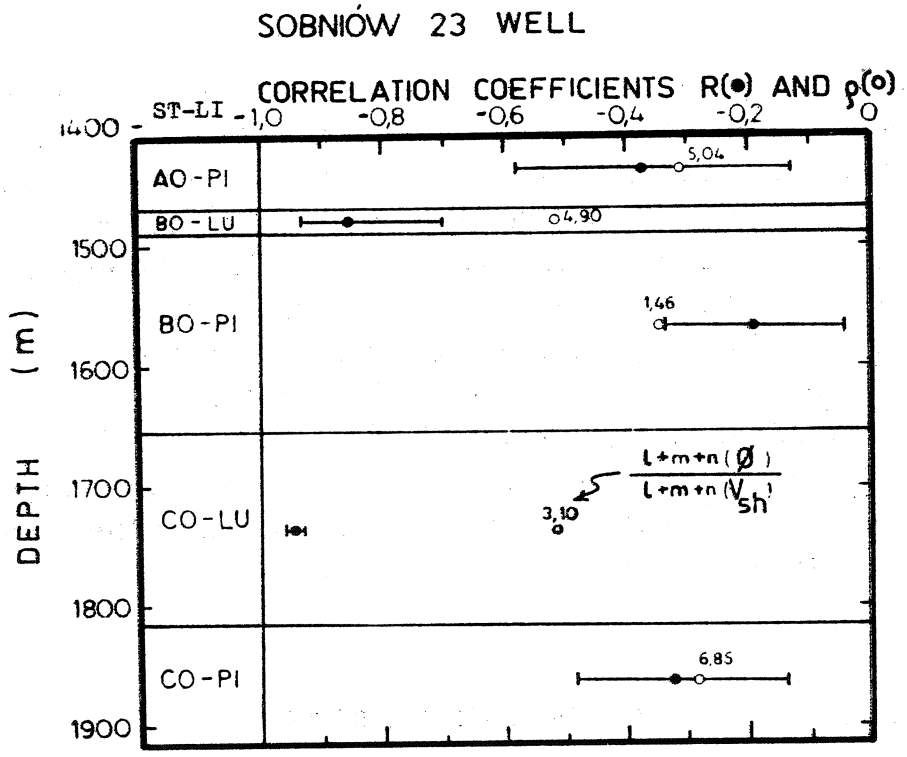

Fig. 29. Comparison of the correlation coefficients R and ϱ obtained for the litho-stratigraphic series in the Sobniów 23 borehole between the log derived porosities and shale contents (cf. Eqs (4.2) and (4.3))

Fig. 29. Porównanie współczynników korelacji R i ϱ pomiędzy wyinterpretowanymi z profilowań wartościami współczynnika porowatości i zailenia dla serii lito-stratygraficznych w otworze Sobniów 23 (patrz wzory (4.2) i (4.3))

with its 95 per cent confidence belts. The results for the Sobniów 23 borehole are given in Fig. 29. The figures above each point representing the ϱ value correspond to the ratio of the (l + m + n) sums for the bivariate distribution which have been estimated independently from the marginal distributions of Ø and V_{sh} using the moment method. As we can see, in the shaly sandstone (marked as PI) there is no evident difference between the ϱ and the R values, whereas in the pure shale (marked as LU) the R values are showing much higher correlation than the p values. On the other hand only for the B sandstone (BO—PI) the bivariate beta distribution is at least admissible (the above mentioned ratio is 1.46), whereas in all other series the joint (Ø,V_{sh}) distribution is far from being the beta one. On the other hand we do not know the accuracy of the estimates of the l, m and n parameters by the moment method used here (we know only that it is not the best one!). As a result we can expect that in the shaly sandstones the intrinsic correlation between the porosity and the shale content does not exist, whereas for the shales does. The approximation, however, of this distribution by the bivariate beta distribution remains still an open question.

5. CONCLUSIONS

The case history presented above can be regarded as an example, how the statistical and the geostatistical treatment of the core sample data can be joined with the same treatment but of the logging data. The general picture of a given geological formation obtained from these two different sources of information is essentially the same. This agreement, however, is valid only when the confidence limits of the estimates are taken into account. This kind of approach is very helpful in the problem of the quantitative interpretation of the well logging data.

We have touched the problem of the joined statistical distribution of the geological parameters. What we have found is that no „a priori" known model of this distribution can be applied and further investigation has to be done in this subject.

6. ACKNOWLEDGMENTS

We would like to express our acknowledgments to the directors of all the three Institutes mentioned on the front page for giving us the opportunity to perform this study.

Thanks are due also to all the persons and/or institutions who/which have supplied us with the necessary geological and radiometric data, namely to Dr. M. Ciechanowska

from the Institute of Gas- and Oil Mining (Cracow) for the sample analysis data, to W. Twaróg from the Cracow's branch of Oil-Mining/Geophysics Company for the logging data, and to the Oil Exploration Companies for the core sample analysis data.

REFERENCES — WYKAZ LITERATURY

Bogacz J., Buniak M., Czubek J. A., Dąbrowski J., Lenda A., Łoskiewicz J., Zorski T. (1979), Geostatistical System of Interpretation of Nuclear Well Logging Data. *Paper presented at the 24-th International Geophysical Symposium*, September 4—7, 1979, Kraków, Poland.

Chayes F. (1971), Ratio Correlation. The Univ. of Chicago Press, Chicago and London.

Czubek J. A., Łoskiewicz J., Gyurcsak J., Lenda A., Umiastowski K., Zorski T. (1977), Geostatistical Method of Interpretation of Nuclear Well Logs. pp. 313—332 in *"Nuclear Techniques in Mineral Resources* 1977", IAEA, Vienna.

Czubek J. A. Zorski T. (1979), Recent Advances in Gamma-Ray Log Interpretation. pp. 45—86 in *"Evaluation of Uranium Resources"*, IAEA, Vienna.

Matheron G. (1965), Les variables régionalisées et leur estimation. Masson et C-ie, Editeurs, Paris.

Zorski T. (1979), FLOZ — The Computer Program for the Primary Interpretation of Nuclear Borehole Logging. *Inst. Nucl. Physics Report* No 1052/AP, Kraków, Poland.